Predicting Spatial Variability in Soil Organic Carbon Among Delmarva Bays

Kinsey Blumenthal

Thesis submitted to the faculty of the Virginia Polytechnic Institute and State University
in partial fulfillment of the requirements for the degree of

Master of Science
In
Geography

James Campbell, Chair
John Galbraith
Megan Lang
Luke Juran

November 17, 2016
Blacksburg, Virginia

Keywords: Soil Carbon, Non-linear Modeling, Topography, Hyperspectral

Predicting Spatial Variability in Soil Organic Carbon Among Delmarva Bays

Kinsey Blumenthal

Abstract

Agricultural productivity, ecosystem health, and wetland restoration rely on soil organic carbon (SOC) as vital for microbial activity and plant health. This study assessed: (1) accuracy of topographic-based non-linear models for predicting SOC; and (2) the effect of analytic strategies and soil condition on performance of spectral-based models for predicting SOC. SOC data came from 28 agriculturally converted Delmarva Bays sampled down to 1 meter. R^2 was used as an indicator of model performance. For topographic-based modeling, correlation coefficients and condition indices reduced 50 terrain-related values to three datasets of 16, 11, and 7 variables. Five types of non-linear models were examined: Generalized Linear Mondel (GLM) ridge, GLM LASSO, Generalized Additive Model (GAM) non-penalized, GAM cubic splice, and partial least-squares regression. Carbon stocks varied widely, 50 to 219 Mg/ha, with the average around 93 Mg/ha. Topography shared a weak relationship to SOC with most attributes showing a correlation coefficient less than 0.3. GLM ridge and both GAMs achieved moderate accuracy at least once, usually using the 16 or 11 variable datasets. GAMs consistently performed the best. Prior to carbon analysis, hyperspectral signatures were recorded for the topmost soil horizons under different conditions: moist unground, dry unground, and dry ground. Twenty-four math treatment and smoothing technique combinations were run on each hyperspectral dataset. R^2 varied greatly within datasets depending on analytic strategy, but all datasets returned an R^2 greater than 0.9 at least twice. Moist unground soil models outperformed the others when comparing the best models among datasets.

Predicting Spatial Variability in Soil Organic Carbon Among Delmarva Bays

Kinsey Blumenthal

Abstract

Delmarva Bays are depressional landforms found throughout the Delmarva Peninsula that provide habitat for a number of endangered amphibian and plant species. Due to the prevalence of these Bays on the peninsula and their location in a highly agriculturalized landscape, many Delmarva Bays have been converted from wetlands into farmland. Whether a Bay is a wetland or agricultural land, organic carbon is an important soil property for a large number of microorganisms and plant health. Increased levels of soil organic carbon (SOC) have been linked with more diversity in soil biota and increased nutrient availability, which affect cropland productivity and ecosystem health. SOC stock and distribution is useful information to help formulate land management practices. However, SOC varies horizontally across a landscape and traditional methods for gathering data are time intensive. This study looked at the potential accuracy of two types of models for predicting SOC variation in agriculturally converted Delmarva Bays: 1) models based on terrain-related attributes, and 2) models based on soil spectral data. Using data collected from 28 agriculturally converted Bays, moderate to high potential accuracy was returned for both types of models. Results suggest terrain-related and spectral-based models may be useful alternatives to traditional soil sampling for looking at SOC variation to inform land management decisions regarding these Bays.

Acknowledgments

I would like to thank my committee for their support, advice, and patience throughout this project. I would also like to specifically thank some others who have greatly contributed to this work: Dr. Greg McCarty and Dr. Valerie Thomas for their help and suggestions; Daniel Fenstermacher for access to his data collected for his thesis work on Delmarva Bays; Ferry Akbar Buchanan and Amy Mallonee for their assistance with field data collection; Steve Nagle for his ability to unfailingly fix the CN Analyzer when it became temperamental; and the statistical consultants at Virginia Tech's Laboratory for Interdisciplinary Statistical Analysis (LISA) for their troubleshooting expertise with R. Lastly, I want to thank my family who are always encouraging and supportive, even when they're on the other side of the world.

This work was made possible by funding from the Virginia Tech Geography Department Poole Fund and the Georgia Pacific Scholarship Fund.

Table of Contents

Abstract (academic)……...ii

Abstract (public)……iii

Acknowledgments ……iv

Table of Contents ……v

List of Figures ……..vii

List of Tables ……...viii

Chapter 1 – Introduction ……..1

Questions ……..…….3

Objectives ……3

Chapter 2 – Literature Review……..4

Wetlands ……...4

Delmarva Bays ……..5

Soil Organic Carbon: Importance and Influencing Factors ……..6

Spatial Variation of Soil Organic Carbon ……7

Spatial Distribution of Soil Organic Carbon in Depressional Wetlands ……...9

Spectroscopy of Soil Carbon ……10

Wetlands ……...12

Chapter 3 – Topographic-based Non-Linear Modeling of Soil Organic Carbon Stocks Among Agriculturally Converted Delmarva Bays ……14

Introduction ……..14

Methods ……15

Field Sampling ……..15

Soil Organic Carbon Analysis ……..16

Bulk Density Pedotransfer Function ……17

Mass Carbon Stock ……...20
Topographically Related Metrics ……21
Carbon–Terrain Analysis ……..25
Collinearity of Variables ……...25
Non-Linear Models ……...26
Results and Discussion ……27
Soil Organic Carbon Variation Among Delmarva Bays ……..27
Collinearity and Variable Selection ……..29
Carbon–Terrain Analysis ……..33
Conclusion ……36
Chapter 4 – Effects of Analytic Strategies and Soil Condition on Spectral-based Predictions of Soil Organic Carbon Among Agriculturally Converted Delmarva Bays ……37
Introduction ……..37
Methods ……38
Spectroscopy ……38
Statistical Analysis ……....39
Results and Discussion ……41
Conclusion ……45
Chapter 5 – Conclusions ……...47
References ……49
Appendix A – Statistics on Pedotransfer Function Training Data ……...53
Appendix B – Correlation Between Terrain Attributes and SOC ...…….55
Appendix C – Correlations of Continuous Terrain Attributes Using Pearson's……57
Appendix D – Correlations of Categorical Terrain Attributes……...……65
Appendix E – Soil Profile Descriptions with Pictures ……..68

List of Figures

Figure 1. Map of study area in the Delmarva Peninsula. Light blue represents the Tuckahoe Creek watershed and dark blue the Upper Choptank River watershed. The watersheds overlap Kent County, DE (outlined in purple), and Talbot, Caroline, and Queen Anne's counties in MD (outlined in orange).……...15

Figure 2. Percentage of soil samples that belong to each soil series…….16

Figure 3. Redoximorphic features found in some of the profiles: soil horizons with heavy redox iron concentration (left), and horizons with oxidized root channels in a depleted matrix (right)…….24

Figure 4. Photo of soil profiles showing the range in soil variation found among the sampled Bays. Markers indicate augered depth in 20 cm increments…….24

Figure 5. Puddling of water in one of the sampled Bays during fieldwork……..39

List of Tables

Table 1. Horizon designations for the bulk density pedotransfer function……..17

Table 2. Number of samples by horizon and texture class……...18

Table 3. Comparison of SOC transformations for modeling training data bulk density…….18

Table 4. Regression model statistics of training before B and BC horizons were combined…..19

Table 5. Regression model statistics of training after B and BC horizons combined……..19

Table 6. Common topographic attributes used to study spatial distribution of SOC……...21

Table 7. Topographically related metrics used in this study……22

Table 8. Summary statistics regarding variation in SOC concentration and horizon thickness of the top most horizons for all sampled points, and variation in SOC stock among sampled Bays……..28

Table 9. Terrain attributes with the reduced datasets of 16, 11, and 7 variables……..31

Table 10. Definitions of the 16 variables from the original reduced dataset and previous soil–landscape modeling studies in which they have been used……..32

Table 11. Previous soil–landscape studies which have used curvature as topographic attributes and the types of curvature examined…….33

Table 12. Statistics for GLM, GAM, and PLSR predictive models of SOC stock. The number of variables that produced the best goodness of fit (R^2) for each model is italicized……34

Table 13. Percent of water present in the samples of the moist dataset……39

Table 14. Effects of math treatments and smoothing on SOC stock predictions of dry ground, dry unground, and moist unground samples. The math treatment of each smoothing technique resulting in the smallest minimum PRESS is italicized for each dataset……..42

1 Introduction

The terrestrial global ecosystem contains a vast quantity of carbon, the majority of which is stored below ground. Natural carbon stores are not evenly distributed across the globe and wetlands hold a disproportionately large share of the world's terrestrial carbon (Lou and Zhou, 2006). However, not all wetlands can store carbon to the same extent and some are even emitters of greenhouse gases like CH_4 and N_2O (Bridgham et al, 2006; Morse et al, 2012). Concerns regarding global climate change and greenhouse gas emissions have fueled research into the role of wetlands in the global carbon cycle. Beyond their potential to store high amounts of carbon, wetlands provide a wide range of environmental, social, and economic functions and services at the local, regional, and global level (Millennium Ecosystem Assessment, 2005). Soil organic carbon (SOC) is crucial for many of these functions as an integral component of soil microbial activity and plant health and development.

A significant body of soil science literature on the spatial distribution of SOC at variety of geographic scales exists, especially pertaining to agriculture. Spatial variation within and among depressional wetlands in the same landscape has been a subject of some study. However, such research tends to involve small sample sizes (less than 10 wetlands) and, when included, oversimplified topography represented by only one or two variables (e.g., Craft and Casey, 2000; Stolt et al., 2001).

Soil–landscape modeling is a method which has been used to study and predict SOC distribution in a number of studies. Through the use of geospatial data some research using soil–landscape analysis has given more detailed attention to topography by including various terrain attributes. Although linear models are commonly used for soil–landscape analysis, non-linear models have been used as well. Some researchers have suggested non-linear models are superior to linear models for simulating the relationship between topography and soil properties

(Thompson et al., 2006; McKenzie and Ryan, 1999). Non-linear models are a large group of statistical analyses, but the generalized linear model (GLM) and random forest have been routinely mentioned as potential models for soil–landscape analysis. However, just as the relationship between topography and SOC distribution cannot be assumed to be the same between regions, the performance of specific non-linear models in predicting SOC using topography may vary depending on geographic location and scale.

Spectroscopy is a second technique widely used to spatially study soil properties like SOC, particularly in agriculture. Despite increased use of spectroscopy to study soil, little research addresses selection of analytic strategies for processing hyperspectral data and potential implications on model performance. The majority of soil spectroscopy research has been conducted in the lab on dry ground soil, but point and imaging spectroscopy record soil under field conditions. Soil spectra under field conditions may be affected by math treatment and smoothing technique to a different extent than dry ground soil. Although this study focused on agriculturally converted Delmarva Bays, most of which are historic wetlands, the findings have implications for spectral research of natural wetland, historical wetland, and upland soils.

As an essential element of soil and plant health SOC is an important factor for general land management in addition to wetland management and restoration. An understanding of SOC distribution and factors affecting its movement are particularly important in agricultural areas where wetlands can be prevalent, but are frequently drained for cultivation, as in the Delmarva Peninsula. The traditional approach of studying SOC distribution solely through collecting and analyzing soil samples in the lab is frequently time and resource intensive. Predictive models of SOC distribution with at least moderate accuracy could provide more timely data for land

management decisions, especially if models are based on more readily available data such as terrain-related attributes or spectra.

Research Questions

(1) To what extent can topographic variables be used to predict SOC variation among depressional landforms in a low relief landscape?

(2) Do analytic strategies for analyzing hyperspectral data and/or the conditions under which soil spectra are recorded affect the performance of spectral-based models for estimating SOC concentration?

Objectives

(1) Determine the variation of SOC levels among agriculturally converted Delmarva Bays;

(2) Identify the relationship of individual topographic attributes to SOC concentration among agriculturally converted Delmarva Bays;

(3) Evaluate the performance of five topography-based non-linear models in estimating SOC stocks among agriculturally converted Delmarva Bays; and

(4) Assess the effect of moisture and particle size on SOC prediction accuracy of hyperspectral data using four smoothing techniques and six math pretreatments on soil samples recorded in three states: moist unground, air dried unground, and air dried ground.

2 Literature Review

2.1 Wetlands

According the U.S. Corps of Engineers (2010), wetlands are defined as being characterized by hydrophytic vegetation, hydric soil, and hydrology sufficient for the first two criteria to occur. However, wetlands are a highly variable category of ecosystem lacking a uniform classification system regarding types of wetlands (Tiner, 2015). Wetlands come in many forms and, as a group, provide a vast array of services at local, regional, and global levels. There are six categories of services and functions provided by wetlands: socioeconomic, water quality, water control, food, habitat, and biogeochemical cycling and storage. Individually, wetlands typically do not perform every function equally as conditions necessary for one service can preclude others (Zedler, 2003; Morse et al., 2012 Brinson and Eckles, 2011).

The USDA is currently engaged in a nationwide Conservation Effects Assessment Project (CEAP) in which one component focuses on wetlands. CEAP–Wetlands aims at gathering and synthesizing existing information on wetlands and conservation practices, and conducting studies to fill in research gaps to better inform conservation decisions regarding wetlands and agricultural areas (Eckles, 2011). CEAP focuses on seven geographic regions, including the Piedmont–Coastal Plain, which includes the Delmarva Peninsula. Wetlands in the Piedmont–Coastal Plain typically provide one or more of the following services: habitat; biodiversity support; enhanced water quality; and greenhouse gas regulation (Brinson and Eckles, 2011). Brinson and Eckles (2011) identifed depressional as a dominate wetland type in their regional synthesis of the Piedmon–Coastal Plain along with riverine and flats (organic-soil and mineral-soil). The role of wetlands in the global carbon cycle forms a topic of particular

interest due to growing concerns regarding global climate change and its link to human-induced and naturally occurring greenhouse gas emissions.

2.1.1 Delmarva Bays

Delmarva Bays are depressional wetlands found only on the Delmarva Peninsula. Morphologically, Delmarva Bays share traits characteristic of Carolina Bays: elliptical shape, sandy rim, and the northwest-southeast orientation of the major axis (Stolt and Rabenhorst, 1987; Fenstermacher et al., 2014). Due to their much smaller size and more circular shape, Delmarva Bays are considered a special subset of Carolina Bays. Likely formed by wind blowouts, Fenstermacher et al. (2014) hypothesize that the peninsula's proximity to the Laurentide Ice Sheet in the Pleistocene indirectly restricted sizes of Delmarva Bays.

In their undisturbed state Delmarva Bays are typically forested, although they can occasionally be found as natural herbaceous ecosystems (Fenstermacher et al., 2014; Stolt and Rabenhorst, 1987). Intensive agricultural activity on the Delmarva Peninsula has led to the conversion of wetlands to farmland on a massive scale by draining the Bays (McCarty et al., 2008; Fenstermacher et al., 2014). Large scale draining of these Bays is contributing to loss of biodiversity through destruction of habitat for endangered amphibian and plant species (Maryland Department of Natural Resources, 2005). The biggest threats to Delmarva Bays are drainage for agriculture, silviculture, and urban development (Tiner et al., 2002). While Delmarva Bays are present throughout the peninsula, they are heavily concentrated in the area near the Maryland-Delaware border that includes the Choptank River watershed (Stolt and Rabenhorst, 1987; Tiner et al., 2002; Maryland Department of Natural Resources, 2005).

Despite their seemingly isolated nature, natural and historic Delmarva Bays have been found to hydrologically connect with other surface waters via ephemeral and intermittent water

channels (McDonough et al., 2015). Extensive drainage ditch networks found throughout the Delmarva Peninsula provide a link between Bays and streams or rivers (McCarty et al., 2008). Ditches provide a constant avenue for the movement of nutrients and sediment from agricultural runoff to other waters, but the use of flow control structures may help reduce the export of some nutrients (McCarty et al., 2008).

2.2 Soil Organic Carbon: Importance and Influencing Factors

SOC is an essential element for vegetation productivity and a large number of soil microorganisms. Benefits of increasing SOC include greater diversity of soil biota and increasing soil nutrient availability. The importance of SOC in crop production, coupled with loss of soil carbon associated with traditional farming practices has made monitoring and evaluation of this soil property of particular importance in agricultural landscapes. A significant portion of agricultural sciences, particularly the conservation agriculture subset, is focused on researching and advocating farming practices less destructive to the soil, including techniques for preserving or increasing SOC. While cropland does have lower SOC stocks than grassland and forest (Murty et al., 2002), there is debate regarding the magnitude of differences. For example, Wiesmeirer et al. (2012) and Wu (2014) argue that the percent decrease in carbon of cropland soils has been routinely over estimated.

Beyond the role SOC plays in maintaining soil and plant health, concerns regarding global warming caused by high carbon dioxide emissions from burning fossil fuel, agriculture, and deforestation have increased attention placed on the role of soil in the carbon cycle (Edenhofer et al., 2014). Ecosystems in which the rate of organic matter entering the soil is higher than the rate of decomposition will increase SOC concentration until equilibrium is reached. Soil is responsible for storing a significant portion of the world's terrestrial carbon

(Batjes, 1996), but is not evenly distributed. Disturbed soils—such as agricultural land—are considered out of equilibrium and therefore have potential to store a larger amount of carbon (Brown, 2016). However, a number of factors may preclude agricultural and other disturbed soils from reaching pre-disturbance carbon levels (Bruce et al., 1999).

With the exceptions of Spodosols, the topmost soil horizons contain the most carbon. Organic carbon in wetlands primarily enters the soil via litter biomass becoming available for use in the soil through decomposition (Lou and Zhou, 2006). According to the detailed account of soil respiration mechanisms and regulators of Lou and Zhou (2006), a number of interconnecting factors impact the rate of decomposition and contribute to spatial variation of soil carbon content. For example, warm temperatures tend to increase decomposition rates by increasing microbial activity, while soil water saturation decreases decomposition rates through limiting availability of gaseous O_2 (Lou and Zhou, 2006).

Wetlands tend to have higher SOC concentration than surrounding uplands, largely because of their distinctive hydrology (Lou and Zhou, 2006). Due to naturally higher capacities of some wetlands to store carbon in the soil, the restoration or creation of wetlands has been suggested as an avenue for helping offset some of a nation's CO_2 emissions. Three caveats of this avenue are that: (1) the restoration and creation of wetlands can be extremely difficult to achieve (Zedler, 2003); (2) disturbed soils can require upwards of a century to reach carbon storage equilibrium (Bruce et al., 1999); and (3) at the same time as wetlands act as net sinks of atmospheric CO_2 they can be net sources of other greenhouse gases, such as CH_4 and N_2O (Bridgham et al., 2006; Morse et al., 2012).

2.3 Spatial Variation of Soil Organic Carbon

A wide body of literature exists examining the spatial distribution of SOC with emphasis

on topographic attributes. In general, topography is correlated with SOC (e.g., Veneteris et al., 2004; Thompson et al., 2006; Schwanghart and Jarmer, 2011). Universal correlations between individual topographic attributes and horizontal spatial distribution of SOC do not exist, and the impact of terrain components can vary within the same landscape decreasing the strength of soil–landscape prediction models (Thompson et al., 2006; Schwanghart and Jarmer, 2011). Spatial variation of soil properties results from a number of compounding factors in addition to topography, including climate, organisms, anthropogenic influence, and geologic activity/history. Land use, land use history, and land management can be particularly strong factors influencing SOC that can overshadow the significance of topography in attempts to understand the spatial distribution of this soil property (Veneteris et al., 2004; Bedard-Haughn et al., 2006).

Incorporation of subsurface water system information has the potential to increase the prediction accuracy of SOC landscape models. Subsurface hydrologic data is notably missing from many such studies (e.g., Veneteris et al., 2004; Thompson et al., 2006; Schwanghart and Jarmer, 2011; Moore et al., 1993; McKenzie and Ryan, 1999; Pastick et al., 2014). In a study of bog microtopography Weltzin et al. (2001) found vertical distance of vegetation from the water table a key determinant in Sphagnum moss productivity—an important component for net increase in SOC. Ju and Chen (2005) found that the inclusion of a hydrological submodel improved a model of soil carbon distribution across Canada's wetlands by simulating soil moisture patterns for different topographic conditions. Conversely, in a study of wetlands across West Siberia, a detailed model of carbon flux and methane emission revealed only very slight differences between a uniform and heterogeneous subsurface water system (Bohn et al., 2013). Despite a lack of significant or definitive differences between the subsurface water system

models, the authors caution dismissal of the heterogenous water table scheme. The findings of these studies regarding what impact, if any, subsurface water plays on SOC spatial variability illustrate the need for such data to be included in more soil–landscape studies. While information concerning subsurface water could provide important additional insight into SOC distribution, it is difficult and time intensive data to collect.

2.3.1 Spatial Distribution of Soil Organic Carbon in Depressional Wetlands

Depressional wetlands are known for their internally uneven distribution of SOC due to their concave shape (Reese and Moorhead, 1996; Craft and Casey, 2000; Bedard-Haughn et al., 2006). Observed variability occurs both horizontally and vertically, with highest SOC levels concentrated in the Bay's center and in the A horizon, respectively (Reese and Moorhead, 1996). The horizontal variation is attributed to: (1) the down slope movement of SOC down basin sides, and (2) the collection of water in the Bay's center. Internal spatial variation in SOC concentration can be clearly evident even in a wetland that is intermittently inundated and/or saturated to the soil surface.

While internal variation of SOC in depressional wetlands is attributed to topography (i.e. shape), focus on connections with vegetation and land use tend overshadow terrain. Stolt et al. (2001) found Palustrine wetlands located at higher elevations had lower SOC levels in Virginia, but no real conclusion could be drawn from the observation. This finding, in conjunction with the lack of a significant relationship between SOC and elevation when wetlands were grouped by vegetation, is by no means conclusive given (1) a sample size of five, (2) the wetlands came from a mix of agricultural and non-agricultural areas, and (3) depressional wetlands may not have been in the study as Palustrine is a large class of wetlands. When independently investigated in different landscapes, land use (Bedard-Haughn et al., 2006) and vegetation (Craft

and Casey, 2000) were found to have a significant correlation with variation in SOC.

In terms of spatial variability of soil carbon among non-bog depressional wetlands, relatively little attention appears to focus on these wetlands and the impact of terrain. However, it should be noted that depressional wetlands are a category of wetland from the hydrogeomorphology classification scheme (Brinson, 1993). Lack of a universal classification method and a tendency of some studies to identify wetlands solely by one feature, such as vegetation type, means it is very likely more research has been done examining SOC and topography among depressional wetlands but it is not readily identified as such.

2.4 Spectroscopy of Soil Carbon

Spectral measurements of soil can be taken at three levels: 1) in the lab (lab spectroscopy); 2) on the ground in the field (point spectroscopy); and 3) via airborne or satellite sensors (imaging spectroscopy). An ever growing body of work also exists on the use of spectroscopy in soil science, particularly with regards to soil carbon. In particular, Croft et al. (2012) provides a comprehensive overview of optical remote sensing techniques used and difficulties faced in the study of SOC and soil organic matter. Numerous spectroscopic studies have been conducted in laboratory settings (and some in the field) demonstrating the use of reflectance data in estimating SOC amounts and their spatial distributions. Remote sensing of soil carbon is typically completed through examination of spectral signatures in the visible and near-infrared portions of the electromagnetic spectrum (Bartholomeus et al., 2008). Mid-infrared spectroscopy can also be used to help predict SOC outperforming near-infrared accuracy and creating more robust models (McCarty et al., 2002; Rossel et al., 2006; McCarty and Reeves, 2006). Despite the better models produced based on this data, mid-infrared remains much less widely used than visible or near-infrared, especially for field data collection, due to the expense

of such sensors.

Through lab spectroscopy, Bartholomeus et al. (2008) demonstrated reflectance in the visible portion of the spectrum (4.0-7.0 μm) decreasing as SOC content increases and the shape of the spectral signature shifting from convex to concave to flat. Lab spectroscopy provides high accuracy estimates of the percentage of organic carbon in soil, but high model accuracy based on these data requires the targeted soil to fall within the soil type and mineralogical range of the spectral indices library used for calibrating/training the data (Bartholomeus et al., 2008). Moisture, shading, and light refracted from other surfaces—a few factors that can be impossible to avoid or control outside the lab—can affect soil spectral signatures and interfere with SOC estimates (Gomez et al., 2008; Croft et al., 2012). Chang et al. (2005) examined effects of soil moisture on near-infrared (NIR) measurements of soil properties, reporting that even small increases in moisture can significantly increase the baseline of the spectral signature and emphasizing signature peaks at 1400nm and 1900nm. Although the NIR prediction models returned different accuracies for carbon estimates between air-dried and moist soil readings, the difference was slight.

Imaging spectroscopy, particularly satellite-based, is less widely used than lab spectroscopy to develop SOC prediction models. Satellite-based models can be highly variable, yielding very low accuracy (Gomez et al., 2008) or high accuracy (Croft et al., 2012), where R^2 is commonly given as an indicator of prediction strength and may not have been validated with outside data. Common caveats of using imaging spectroscopy include greater preprocessing requirements, spatial resolution limitations, and atmospheric interference. These drawbacks are compounded when the objective is to gather information on soil properties but vegetation cover mixes with or completely obscures the soil signature. Imaging spectroscopy, where the aim is to

study or estimate soil properties, is rarely used outside agricultural areas or other geographic regions where vegetation is sparse.

2.4.1 Wetlands

Extensive literature exists on remote sensing in wetland studies, and on remote sensing of carbon in wetlands. Increasingly remote sensing is used to study wetlands and, in particular, estimate wetland carbon storage. However, remote sensing study of wetland carbon is almost exclusively confined to above-ground storage. Use of remote sensing to study soil properties is generally limited to open or sparsely vegetated areas, which is likely why so few wetland studies attempt to use such data to study subsurface carbon storage.

As a result, very few studies employ spectroscopy to examine wetland soils despite potential benefits of such an approach. Bouchard et al. (2003) found NIR reflectivity taken over the winter useful in predicting carbon and nitrogen content of leaf litter in salt marshes. VIS and NIR-based chemometric models are effective predictors of a number of soil properties, including carbon (Cohen et al., 2005). Cohen et al. (2007) found VIS and NIR lab spectroscopy of wetland soils from three different ecoregions effective predicting the phosphorous absorption capacity of wetland soils.

Most carbon studies in vegetated areas involving soil are closer to the strategy applied by Suchenwirth et al. (2012) which considered estimated carbon as a combination of that stored in the soil and of biomass. A non-exhaustive account of imaging spectroscopy of soil carbon provided by Anne et al. (2014) illustrates the large number of studies carried out on this subject.

Due to relationships between moisture and soil carbon, inundation, saturation, and soil moisture can be used as proxy measurements of SOC. Inherent in the total carbon estimate approach of Suchenwirth et al. (2012) is the assumption that a strong relationship exists between

vegetation types and SOC. The study by Anne et al. (2014) using Hyperion and Landsat TM imagery to detect and differentiate stable and labile carbon found a correlation between carbon and vegetation spectra, thereby supporting the idea that soil properties and vegetation spectral reflectance may be related. While hyperspectral models were successful in modeling both forms of carbon, there is a wide range of accuracies among the models generated. Although their focus was upon phosphorous, Rivero et al. (2007) found that inclusion of satellite-derived spectral indices from vegetation in a geospatial model of environmental variables returned higher prediction accuracy on the spatial distribution of soil phosphorous in the Florida Everglades. The applicability of this method for studying other soil properties remains in question.

While the presence of dense vegetation can impede use of imaging spectroscopy, not all wetlands feature dense plant growth. Point spectroscopy could be used as a less destructive and quicker method for gathering soil data from wetlands that allows for more intensive sampling of vulnerable ecosystems. Field and lab based studies of wetland soils, while useful on their own, could be used to create spectral libraries to increase prediction accuracy of imaging spectroscopy-based models.

3 Topographic-based Non-Linear Modeling of Soil Organic Carbon Stocks Among Agriculturally Converted Delmarva Bays

3.1 Introduction

Delmarva Bays are a dominant feature of the Eastern Shore found throughout the peninsula. While estimates regarding the number of Delmarva Bays vary widely, the latest estimate based on LiDAR data is around 17,000 in the Maryland and Delaware sections of the Delmarva Peninsula (Fenstermacher et al., 2014). Due to the highly agricultural nature of the Delmarva Peninsula the majority of Delmarva Bays has been converted into crop- and pasture land. While some studies have been done on Delmarva Bays and soil carbon, they have focused on the internal variation of soil carbon. Variation of soil carbon stock among the Bays has yet to be examined.

Spatial variation of soil carbon at the field level has been the focus of a number of studies in and around the Delmarva area. Higher concentrations of soil carbon are typically confined to lower areas in the fields, which for sites located on the Eastern Shore may be agriculturally converted Bays. ('Agriculturally converted bays' refers to Delmarva Bays which are currently being used for cropland. Agriculturally converted Bays may or may not be prior converted croplands as defined in Section 514.30 of the National Food Security Act Manual in which wetlands have been altered and used for commercially growing crops prior to December 23, 1985 (USDA Natural Resources Conservation Service, 2010)). Attempts have been made to link specific topographic factors with soil carbon distribution, but all correlation found so far has been weak and poorly performing topography based predictive models have resulted (e.g., Veneteris et al., 2004; Hively et al., 2011).

While Veneteris et al. (2004) used linear modeling they suggested the use of non-linear models as a potential avenue for predictive modeling in low relief environment. Linear models

are most commonly used (Veneteris et al., 2004; Schwanghart and Jarmer, 2011; Moore et al., 1993), but non-linear models have been used and suggested by others as a superior means for simulating the relationship between topography and soil properties (Thompson et al., 2006; McKenzie and Ryan, 1999). This study focused on agriculturally converted Delmarva Bays and aims to: (1) determine the variation in SOC stock among these Bays, (2) examine the relationship between terrain-related attributes and SOC stock in Bays, and (3) assess the performance of five non-linear models to predict SOC stocks among Bays.

3.2 Methods

3.2.1 Field Sampling

Field sampling took place over the last two weeks of December 2015 in the Maryland portion of the Upper Choptank River watershed (Figure 1). Prior to fieldwork, Delmarva Bays were identified based on their morphology using LiDAR-derived DEMs of the area. For the sake of accessibility, Bays of interest were confined to those on properties owned by people who had had previously granted site access for USDA related studies. Twenty-eight Bays from six properties were sampled.

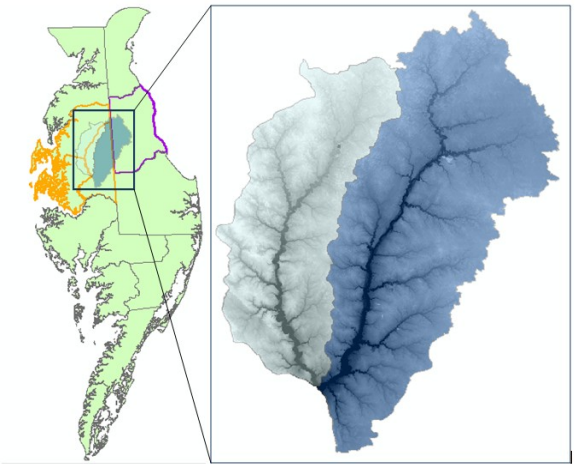

Figure 1. *Map of study area in the Delmarva Peninsula. Light blue represents the Tuckahoe Creek watershed and dark blue the Upper Choptank River watershed. The watersheds overlap Kent County, DE (outlined in purple), and Talbot, Caroline, and Queen Anne's counties in MD (outlined in orange).*

Soil was sampled down to one meter at three spots in each Bay using a 3.25 inch diameter bucket auger. Three points within each basin were arbitrarily selected for sampling. Major soil horizons were identified and one or two samples taken of each one for later carbon analysis. Two samples were taken from A horizons thicker than 20 cm (one near the top and one near the bottom). The percentage of SOC for these samples was then averaged to give a more accurate representation of the horizon's carbon. The depth to freestanding water, if encountered, was also recorded. A total of 350 horizons were recorded for the 84 sampled pedons. Eleven soil series were sampled in all with over half coming from three series, Lenni, Ingleside, and Woodstown (Figure 2). Soils were predominately clay loam.

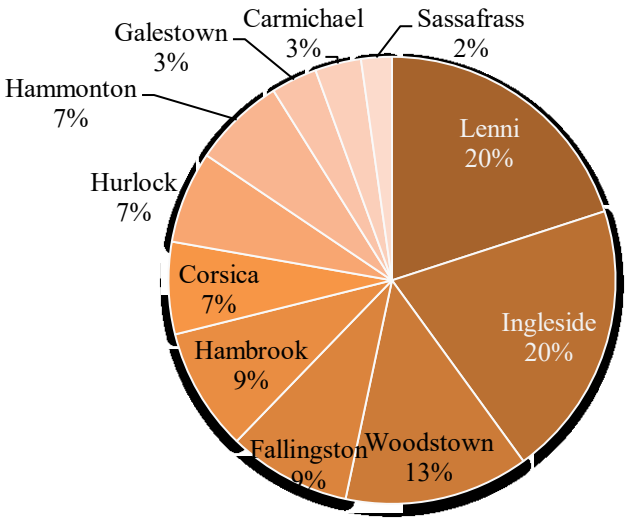

Figure 2. *Percentage of soil samples that belong to each soil series.*

3.2.2 Soil Organic Carbon Analysis

All soil samples were air dried, powder ground, and run through a 2 mm sieve before analysis. Total carbon and total organic carbon were determined via combustion analysis using a VarioMax CN Elemental Analyzer. To convert SOC from point data to carbon stock a pedotransfer function (PTF) was utilized to obtain bulk density.

3.2.2.1 Bulk Density Pedotransfer Function

Organic carbon/organic matter, soil texture, and depth are generally considered to be the biggest factors affecting bulk density. A bulk density pedotransfer function (PTF) for the study area's region was created based on training data gathered from Fenstermacher (2011) and the NRCS National Soil Service database. Only horizons from soil series sampled in this study and accompanied by SOC data were included. From the data available for use as the training dataset four horizons were discarded as outliers in relation to horizons collected in this study—O, 2Bx, Bhs, and ^AC. A horizons situated directly below Ap horizons generally have higher bulk density than other A horizons. As the only A horizons found in the data collected for this study were directly below an Ap horizon, all A horizons not directly under an Ap horizon were excluded from the training data. All horizons missing SOC data were also excluded. As only four horizon classes were present in the data collected during this study the horizon designation groups were largely confined to divisions by major soil horizon and t horizons. The remaining 161 horizons of the training data were consolidated into seven horizon designation classes (Table 1). The training dataset and this study's data were grouped by horizon class into three soil texture groups—sand, clay, and loam (Table 2).

Table 1. *Horizon designations for the bulk density pedotransfer function.*

Consolidation of Horizons Sampled in Previous Studies	Horizons Sampled in this Study
Ap: Ap, Ap1, Ap2 **A or AB:** A, 2A, A1, A2, A3, Ab1, Ab2, Ag, AE, AB, ABg, A/B **CB + C:** C, C1, C2, Cg, Cg2, 2C, CB, CBg, 3CBg **BC:** BC, 2BC, BCg, BCg1, BCg2, 2BCg **B:** B, Bg, Bg1, Bg2, Bg3, 2Bg, 2Bg2, 3Bg3, 2Bg3, Bgb1, Bw, Bw1, Bw2, Bw3, 2Bw'2, 3Bw'3 **Bt + BCt:** Bt, Bt1, Bt2, Bt3, Btg, Btg1, Btg2, Btg3, 2Btg1, 2Btg2, BCt, 2BCt, BCtg **E:** E, Eg, EB, E/A	**Ap:** Ap, Ap1, Ap2 **A** **B:** B, B1, B2, B3, Bg, Bg1, Bg2, Bg3 **Bt:** Bt, Bt1, Bt2, Btg, Btg1, Btg2, Btg3, Btg4

Table 2. *Number of samples by horizon and texture class*

Training Data	**Number of Horizons**				**This Study's Data**	**Number of Horizons**			
	Texture					Texture			
Horizon	S	L	C	Total	Horizon	S	L	C	Total
Ap	0	43	0	43	Ap	1	92	0	93
A or AB (directly under Ap)	0	5	0	5	A	1	56	0	57
B	13	46	1	60	B	14	114	0	128
Bt + BCt	7	29	2	38	Bt	0	94	0	94
BC	12	4	0	16					
CB + C	7	5	0	12					
E	2	3	0	5					

Bulk density and SOC mean and standard deviation were calculated for each horizon by texture group. Analyses were run in RStudio version 3.3.1. When SOC is used in a bulk density PTF regression it is usually transformed using a log or square root (see De Vos et al. (2005, p.502) and Kaur et al. (2002, p. 852) for tables listing equations used in various studies). Untransformed, log10, ln, and square root SOC were run in single regression models for bulk density and the best method selected (Table 3). Square root was the best SOC transformation based on root mean squared error (RMSE) and R^2 value. To determine correlation of horizon, texture class, depth (to middle of horizon), and SOC with bulk density, a number of additional regression models were run (Table 4). SOC and depth were the only variables of significance.

Table 3. *Comparison of SOC transformations for modeling training data bulk density.*

Regression Models (B and BC separate)	**Multiple R^2**	**Adjusted R^2**	**RMSE**	**Significant variables (p<0.05)**
lm(BulkDensity ~ SOC)	0.45	0.45	0.13	SOC
lm(BulkDensity ~ sqrtSOC)	0.48	0.48	0.13	sqrtSOC
lm(BulkDensity ~ LnSOC)	0.41	0.40	0.14	LnSOC
lm(BulkDensity ~ Log10SOC)	0.41	0.40	0.14	Log10SOC

Table 4. *Regression model statistics of training before B and BC horizons were combined*

Regression Models (B and BC separate)	Multiple R^2	Adjusted R^2	RMSE	Significant variables (p<0.05)
lm(BulkDensity ~ sqrtSOC)	0.48	0.48	0.13	sqrtSOC
lm(BulkDensity ~ Texture)	0.04	0.03	0.18	None
lm(BulkDensity ~ Horizon)	0.08	0.04	0.17	None
lm(BulkDensity ~ Depth)	0.09	0.09	0.17	Depth
lm(BulkDensity ~ sqrtSOC + Depth)	0.50	0.49	0.13	sqrtSOC Depth

Due to the similarity in bulk density and SOC, the BC and B horizons of the training data were combined and the regression models were run again (Table 5). The consolidation of horizons resulted in lower R^2 values and higher RMSE except for SOC and the combined SOC and depth model. The PTF for predicting bulk density selected for this study was the multiple regression using SOC and depth based off the B and BC consolidation of the training data.

Table 5. *Regression model statistics of training after B and BC horizons combined*

Regression Models (B and BC separate)	Multiple R^2	Adjusted R^2	RMSE	Significant variables (p<0.05)
lm(BulkDensity ~ sqrtSOC)	0.51	0.51	0.13	sqrtSOC
lm(BulkDensity ~ Texture)	0.04	0.02	0.18	None
lm(BulkDensity ~ Horizon)	0.07	0.05	0.18	None
lm(BulkDensity ~ Depth)	0.09	0.08	0.18	Depth
lm(BulkDensity ~ sqrtSOC + Depth)	0.54	0.53	0.12	sqrtSOC Depth

While SOC is widely acknowledged as being strongly correlated with bulk density, efforts were made to increase prediction accuracy of the bulk density PTF by incorporating horizon designation and soil texture class. Run individually and as part of a standard multiple linear regression, horizon class and texture group were not significant factors in predicting bulk density. In working to create a model for predicting bulk density in pedons when the bulk density of some horizons were missing and SOC data unavailable, Sequeira et al. (2014) used variables

including soil textural class and horizon designation in a random forest model. For their model predicting bulk density, textural class and horizon were found be the second and fourth most important variables, respectively. However, known bulk density of some horizons within the pedon of interest was by far the strongest factor in determining the missing values. Random forest was not applicable for use in the current study given the small data size. The use of percent sand and percent clay may have increased the prediction accuracy of the model, but such lab determined data was missing from much of the training data and only tactile determination of soil class was done for the data gathered in this study due to time constraints.

Prediction power of the selected model had a mean square error of 0.016 using leave-one-out cross-validation (cv.lm function of the 'DAAG' package set with folds equal to the number of observations). Application of the PTF to this study's data could not be validated against measured bulk density. Accuracy of bulk density predictions for this study's data were not assumed to be significantly lower than the cross validation results of the training data given (1) the training data used to build the PTF came from the same region, and (2) there were similar distribution ratios of horizon and texture class between the two datasets.

3.2.2.2 Mass Carbon Stock

In order to estimate the mass of carbon within each Delmarva Bay the percent SOC by weight was converted into Mg/ha for each sampled point using equation one from Wiesmeier et al. (2012) where volumetric fraction of rock fragment is zero:

$$\text{SOC Stock (Mg/ha)} = \sum_{i=1}^{n} \text{SOC concentration} \times \text{BD} \times \text{depth} \qquad \text{[EQ.1]}$$

Where n is the number of soil horizons identified and sampled, SOC concentration is in g/kg, BD is bulk density in g/cm^3, and depth is horizon thickness in cm. The SOC stock for each Bay was calculated as the average of the three points sampled within the basin.

3.2.3 Topographically Related Metrics

LiDAR-derived DEMs for the Maryland counties containing the Upper Choptank River watershed were obtained from MD iMap, sinks were filled to create a depressionless DEM, and drainage ditches were masked. Due to the extensive research conducted on SOC and topography a wide range of terrain parameters have been incorporated to study this correlation. Commonly used topographic attributes relevant to this study are listed in Table 6. Due to this study's focus on depressional wetlands, additional variables to those in Table 6 were examined. All topographically related metrics used in this study are listed in Table 7.

Table 6. *Common topographic attributes used to study spatial distribution of SOC.*

Topographic Attributes	Studies
Curvature - **Profile** - **Planar** - **Tangential** - **Total**	*Moore et al. (1993);* *McKenzie and Ryan (1999);* *Veneteris et al. (2004);* *Thompson et al. (2006);* *Schwanghart and Jarmer (2011)*
Wetness Index - **Topographic Wetness Index (TWI)**	*Moore et al. (1993);* *Veneteris et al. (2004);* *Thompson et al. (2006);* *Schwanghart and Jarmer (2011);* *Pastick et al. (2014)*
Slope/Gradient	*Moore et al. (1993);* *McKenzie and Ryan (1999);* *Veneteris et al. (2004);* *Thompson et al. (2006);* *Schwanghart and Jarmer (2011);* *Pastick et al. (2014)*
Slope length/Flow length	*Moore et al. (1993);* *Veneteris et al. (2004);* *Thompson et al. (2006);* *Schwanghart and Jarmer (2011)*
Elevation	*Moore et al. (1993);* *McKenzie and Ryan (1999);* *Thompson et al. (2006);* *Pastick et al. (2014)*
Upslope Area/(Specific) Catchment Area	*Moore et al. (1993);* *McKenzie and Ryan (1999);* *Thompson et al. (2006);* *Schwanghart and Jarmer (2011)*

Table 7. *Topographically related metrics used in this study.*

Categorical Data	Continuous Data
Known Drainage	Bay Area (BA)
Covered Drains	Average Basin Elevation
Pipes	Bay Slope Maximum
Tile Drains	Ditch Width Average
Ditches	Ditch Depth Average
Redox Iron Concentrations	Upslope Catchment Area (UCA)
Grey Redox Depletions	Upslope Catchment Area to Bay Area Ratio (UCA:BA)
Free Standing Water	Aquifer Thickness (max, min, mean)
Samples Soil Series	Upslope Catchment Area (min, max, mean)
	Upslope Catchment Area Maximum Flow Length
	Upslope Catchment Area Curvature (min, max, mean):
	- Total, planar, platform, tangential
	Bay Curvature (min, max, mean):
	- Total, planar, platform, tangential
	Topographic Wetness Index (TWI)
	Terrain Characterization Index (TCI)
	NDVI (min, max, mean)

The following terrain metrics were calculated from a depressionless DEM using ESRI's ArcGIS version 10.3: Bay area, elevation, width and depth of ditches, upslope catchment area, upslope catchment area to basin area ratio, slope, upslope flow length, curvature of Bays and curvature of upslope area (total, planar, platform, and tangential), topographic wetness index (TWI), and terrain characterization index (TCI). Tangential curvature was calculated using equation two following Thompson et al. (2006):

$$K_t = K_c \times S \qquad \text{[EQ. 2]}$$

Where K_t is the tangential curvature, K_c is the planar curvature, and S is the slope in percent.

TWI is the most common wetness index used in studies of soil carbon distribution as a ratio of specific catchment area to slope following equation three from Beven and Kirkby (1979):

$$TWI = \ln\left(\frac{\alpha}{\tan\beta}\right) \qquad \text{[EQ. 3]}$$

Where α is the specific upslope catchment area and β is the slope (in percent). TCI, though less commonly used than TWI, was included in this analysis following the study by Thompson et al.

(2006) that found TCI to be negatively correlated with soil organic matter. TCI is an estimate of soil transport capacity using equation four from Park et al. (2001):

$$TCI = \ln(\alpha) \times K \quad \text{[EQ.4]}$$

Where α is the specific upslope catchment area and K is total curvature.

Additional topographically related metrics not derived from the DEM included in the analysis were normalized difference vegetation index (NDVI); aquifer thickness; known drainage; type of drainage; soil series; and presence or absence of redox iron concentrations, grey redox depletions, and free standing water within the first meter. NDVI is a measure of photosynthetic activity (greenness), which is affected by a number of factors including water availability. NDVI was included to assess its use in predicting SOC levels as an indicator of Bay wetness under the assumption that wetter Bays contain a higher concentration of SOC. While NDVI is not frequently used as a predictor of soil properties its use is not unprecedented (e.g., McKenzie and Ryan, 1999). NDVI was calculated in ESRI's ArcGIS version 10.3 from 2013 NAIP imagery of the study area.

Although a hydrologic study of the subsurface water system was beyond this study, an aquifer thickness map for the Delmarva Peninsula was recently made available for use in this research. The map is a raster layer of the thickness of the unconfined surficial aquifer underlying the Delmarva Peninsula (Denver and Nardi, 2015). Thickness refers to the difference between the surface of the land and the bottom of the aquifer.

Seven basins had clear evidence of a drainage system: four had ditches, and three had covered drains leading to subsurface pipes situated at the basins' lowest point. Water was found within the first meter in seven Bays, but only four of these had visible signs of artificial drainage.

Seventy of the 84 total soil profiles taken had redoximorphic iron concentrations within the first meter (Figure 3). Seventy-eight profiles had grey redoximorphic depletions within one meter. While redoximorphic features are indicative of long-term, long-duration water table height, absence of these features is not proof hydrologic flux does not bring water into the first meter. The duration of time the water table is elevated may be shorter than needed to produce redoximorphic features. A wide rang in diversity was seen in the soil profiles among the Bays sampled for this study (Figure 4).

Figure 3. *Redoximorphic features found in some of the profiles: soil horizons with heavy redox iron concentration (left), and horizons with oxidized root channels in a depleted matrix (right).*

Figure 4. *Photo of soil profiles showing the range in soil variation found among the sampled Bays. Markers indicate augered depth in 20 cm increments.*

3.2.4 Carbon–Terrain Analysis

Although linear regression tends to be the most widely used method for soil–landscape modeling, models that can handle nonlinear data may produce more accurate predictions (Thompson et al., 2006). Veneteris et al. (2004) found no strong correlation between topographic parameters and SOC concentration in agricultural fields situated within a low relief area using stepwise regression and suggested non-linear modeling may yield different results. Generalized linear models (GLM) have been used to model spatial predictions of soil properties—including carbon—with respect to a wide range of environmental factors (McKenzie and Ryan, 1999), and have been mentioned as a model with potential for studying the relationship between soil properties and topography (Thompson et al., 2006). While GLM has been explicitly mentioned, a number of non-linear statistical models exist that may prove useful in predictive modeling of soil.

3.2.4.1 Collinearity of Variables

As a high level of correlation was expected to be present in the terrain attributes, especially among the curvature variables, correlation analysis and condition index (CI) were run. All analyses were carried out using RStudio version 3.3.1 software. Correlation analyses were performed to assess the strength and direction of the relationship among the 50 terrain attributes and between each terrain attribute and Bay carbon stock. Due to the mix of continuous and non-continuous data Pearson's and Spearman's rank correlation coefficients were used with a standard 0.05 p-value. The extent of multicollinearity in the terrain data was assessed using the CI (colldiag function of the 'perturb' package). Collinearity usually refers to the presence of two or more variables that are measurements of the same hidden variable (Dormann et al., 2013). The presence of highly correlated variables can adversely affect model predictions by over

emphasizing some variables and masking the importance of others. While correlation is different referring to interdependence between variables, high correlation between variables can be interpreted as collinearity (Dormann et al., 2013). In this study high correlation was assumed to indicate high collinearity due to use of variables which were all terrain attributes or were related to topography.

A cluster-independent method of removing sources of high collinearity among the independent variables prior to analysis was used based on methods discussed by Dormann et al. (2013). Two maximum CI thresholds, 30 and 10, were used to identify significant collinearity among the examined variables, and a maximum absolute value of correlation coefficient threshold of 0.7 ($|r|>0.7$) was used. First, correlation coefficients were used to reduce the original 50 variables down to 16. Then, CI was run on these 16 to get two more reduced datasets (one using a CI threshold of 30 and one using 10).

3.2.4.2 Non-Linear Models

The selected four datasets of variables were used using five non-linear models: GLM with LASSO regularization, GLM with ridge regularization, generalized additive model (GAM) with no penalization, GAM with cubic splice, and partial least squares regression (PLSR). LASSO and ridge regularization were run for comparison of the GLM since LASSO can perform variable selection and ridge is more resistant to collinearity. Due to the flexibility of GAM and its ability to overfit data, an unpenalized and cubic spliced version of this model was run for comparison. All models were validated using leave-one-out cross-validation.

GLM, GAM, and PLSR were selected for comparison due to their ability to model non-linear relationships and varying robusticity to highly collinear data (see Dormann et al. (2013) for an overview of correlation, collinearity, and their effects on non-linear predictive models).

Models were compared based on goodness of fit (R^2) and root mean square error (RMSE) calculated using the following equations:

$$R^2 = 1 - \left[\frac{\sum(y_i - \hat{y}_i)^2}{\sum(y_i - \bar{y})^2}\right] \quad \text{[EQ. 5]}$$

$$RMSE = \sqrt{\frac{\sum(y_i - \hat{y}_i)^2}{n - 3}} \quad \text{[EQ. 6]}$$

Where y_i is the observed SOC stock concentration, $\hat{y}_i$ is the predicted SOC stock concentration, $\bar{y}$ is the mean of the observed SOC stock concentration, and n is the number of observations. The number of components for PLSR was selected based on the minimum PRESS statistic. GLM predictions were generated based on the minimum lambda. For the purpose of this study R^2 was used as an indicator of each model's predictive strength so that performance among models could be compared. While all R^2 values were the product of leave-one-out cross validation, data from all sampled Bays were used as model inputs. As a result, no verification of actual accuracy of predictions for Bays outside the 28 sampled for this study could be calculated.

3.3 Results and Discussion

3.3.1 Soil Organic Carbon Variation Among Delmarva Bays

Overall concentration of SOC within the first meter ranged from 0.25% to 2.2%, using a weighted average for differences in horizon thickness. In general, the top horizon contained the greatest concentration of carbon. The difference in carbon concentration between the top horizon and the horizon with the greatest percentage of carbon was less that 0.90% for all but four profiles. There were eight sample locations (5 Bays) in which the top horizon did not contain the highest concentration of SOC. Low SOC concentration within the first meter was found for these eight sample locations (17.8–39.3%). Even including these eight points, on average, approximately 50% of the SOC stock within the first meter was situated in the top horizon for

the 28 sampled Bays (Table 8). SOC stocks among the sampled Bays varied widely ranging from approximately 50 Mg/ha to 219 Mg/ha. The range in carbon stock falls within that found by Fenstermacher (2011), but the mean in this study is substantially lower—93 Mg/ha compared to 200 Mg/ha. The higher mean found by Fenstermacher (2011) is unsurprising given that study's inclusion of natural Delmarva Bays and that decreases in carbon are associated with land conversion to agriculture.

Table 8. *Summary statistics regarding variation in SOC concentration and horizon thickness of the top most horizons for all sampled points, and variation in SOC stock among sampled Bays.*

	SOC within Top Horizon (% of SOC stock within first meter)	Top Horizon Thickness (cm)	Average SOC Stock (Mg/ha)
Minimum	18.5	13	49.5
Maximum	83.4	53	219.2
Mean	49.8	25	93.2
Median	46.6	20	84.8
Standard Deviation	15.6	8	41.3
Range	64.8	40	169.6

Bays sampled in this study range in size, but variation in SOC stock can only be partly attributed to differences in Bay area. A Pearson's correlation of 0.3 was found between Bay area and SOC stock, where SOC stock is the average from the three sampled points within each Bay and reported as SOC per unit area (Mg/ha) based on a 54.11 cm^2 sampled area for each point. The Bays sampled for this study had areas ranging from 0.44 ha to 3.52 ha with a mean of 1.58 ha and standard deviation of 0.82 ha making it representative of the majority of Delmarva Bays in terms of size (Fenstermacher et al., 2014). There was one extreme outlier with an area of 9.82 ha formed from the overlap of at least three Bays. The three Bays with the highest SOC stock—219.2 Mg/ha, 132.4 Mg/ha, and 114.6 Mg/ha—were all ones in which the highest concentration of SOC was found below the topmost soil horizon at two or more of the Bays' sample locations. While Weismeier et al. (2012) found sample depth in agricultural land to affect soil carbon estimates, their advocacy for sampling down to the parent material and measuring all soil

parameters is an idealized method for determining 'true' soil carbon stock. Sampling down to the parent material is impractical for areas like the Delmarva Peninsula where the C horizon is more than two meters below the ground surface (Fenstermacher, 2011). Although the carbon stock estimates in this study are based on samples that did not reach the parent material, samples were taken down to one meter where the majority of soil carbon is stored (and approximately the same depth where the parent material began at the Weismeier et al. (2012) study site).

3.3.2 Collinearity and Variable Selection

Using the results of Pearson's correlation coefficient, the 24 curvature variables were pared down to eight (one variable for Bay and upslope area total, planar, profile, and tangential curvature). Minimum bay tangential curvature was the first variable selected because it had the strongest relationship to Bay SOC stock. The remaining seven curvature variables were selected in descending order of the strength of their correlation to bay SOC stock. Selection of the variable was also contingent on an absence of a strong correlation ($|r|\geq 0.7$) with previously chosen variables. A CI was run after the eight curvature variables were chosen to assess multicollinearity. The CI was over 30 (the maximum value for collinearity), but fell under the threshold with removal of the minimum Bay profile curvature.

A number of the categorical data are highly correlated to a number of other terrain attributes, but had very little relationship to Bay SOC stock. Only two of these variables—known drainage and ditches—have a strong relationship with SOC stock at or over the desired 95% confidence interval. Known drainage was chosen over ditches for its higher correlation to SOC stock and strong relationship with a number of excluded variables. Lacking significant correlation with known drainage and the rest of the terrain attributes, maximum aquifer thickness was selected to represent subsurface hydrology due to a greater correlation to SOC stock than

found for the minimum or average. All aquifer values had weak negative correlation with SOC stock suggesting either aquifer thickness has little influence on soil carbon or the estimates of aquifer thickness were not calculated at a scale that makes this data meaningful for this type of Bay level analysis.

Based on 2013 NAIP taken over the summer, maximum NDVI is positively correlated with Bay SOC stock. Minimum NDVI and average NDVI are both negatively correlated with Bay SOC stock. While rainfall can vary significantly even over relatively small areas, reception of precipitation was assumed to be equivalent for all Bays. Of the three NDVI value, average Bay NDVI was chosen for inclusion in the models due its higher correlation to Bay SOC stock.

TWI and TCI are highly correlated with TCI chosen for inclusion in the analysis due a slightly stronger correlation to Bay SOC stock and the high correlation between TWI and the average Bay planar curvature. Bay area (BA), upslope catchment area (UA), and the UA to BA ratio do not have high correlation with SOC stock. Despite the higher r value of Bay area with SOC stock the UA to BA ratio was selected under the assumption higher values for this variable are linked to a higher volume of surface water runoff from precipitation entering the Bay relative to Bay size and hence greater SOC stock. Maximum flow path was excluded due to strong correlation with UA to BA ratio and a weak relationship to SOC stock. Both Bay slope variables were removed due to high correlation with curvature variables that had stronger relationships to SOC stock. Bay slope maximum was selected over Bay slope average due to a higher correlation with SOC stock. Ditch depth average was selected over ditch depth width for the same reason.

With this refined data set of 16 variables (Table 9), a CI was run before proceeding with the carbon–terrain analysis. As the CI returned high values (>80) variables, all attributes weighted more than 0.7 for CI's over 30 were removed and the CI run again. This process was

repeated until the highest CI fell below 30 with 11 variables remaining. Variables continued to be removed in this method until the highest CI fell below 10 with 7 attributes left (Table 9).

Table 9. *Terrain attributes with the reduced datasets of 16, 11, and 7 variables.*

16 Variables	11 Variables	7 Variables
Ditch Depth Average (m)	Ditch Depth Average (m)	Ditch Depth Average (m)
Elevation (m)	Upslope Area to Bay Area ratio	Upslope Area to Bay Area ratio
Upslope Area to Bay Area ratio	Bay Slope Max (percent rise)	Upslope Total Curvature Average
Average NDVI	Upslope Total Curvature Average	Upslope Profile Curvature Average
Max Aquifer Thickness (m)	Upslope Profile Curvature Average	Bay Planar Curvature Average
Bay Slope Max (percent rise)	Bay Total Curvature Max	Upslope Flow Path Length Max
Upslope Total Curvature Average	Bay Planar Curvature Average	Known Drainage
Upslope Planar Curvature Max	Bay Tangential Curvature Min	
Upslope Profile Curvature Average	TCI Average	
Upslope Tangential Curvature Max	Upslope Flow Path Length Max	
Bay Total Curvature Max	Known Drainage	
Bay Planar Curvature Average		
Bay Tangential Curvature Min		
TCI Average		
Upslope Flow Path Length Max		
Known Drainage		

Most of the resulting variables in the refined datasets have been used in previous soil–landscape models. Definitions of the 16 variables are provided in Table 13. Some studies that have used these 16 variables are listed in Table 10 and 11. Four of the 16 variables were not used in any of the soil–landscape studies reviewed in Tables 10 or 11: upslope area to Bay area ratio, maximum aquifer thickness, ditch depth average, and known drainage.

Upslope area to Bay area ratio was not explicitly used in the studies examined here, but catchment area was a common input (refer back to Table 6). Given the focus of this study on topographically enclosed depressional landforms upslope catchment area to Bay area ratio was considered to provide catchment area data that were normalized for basin area. As discussed in the previous chapter, data on subsurface water is commonly missing from soil–landscape modeling, but has the potential to increase model predictive accuracy. In the absence of hydrologic groundwater data, aquifer thickness, ditch depth, and known drainage were used to provide information on Bay wetness and the relationship of the Bays to groundwater. Aquifer

thickness of the surficial aquifer was used in place of depth to the top of the surficial aquifer (from the ground surface) as this data was unavailable for the sampled Bays.

Table 10. *Definitions of the 16 variables from the original reduced dataset and previous soil–landscape modeling studies in which they have been used.*

16 Variables	Definition	Previous Studies
Elevation	Bay basin height above sea-level	*Moore et al. (1993); McKenzie and Ryan (1999); Thompson et al. (2006) Pastick et al. (2014)*
Upslope Area to Bay Area Ratio	Ratio of upslope catchment area to Bay area	
Average NDVI	Average NDVI of Bay (excluding ditches)	*McKenzie and Ryan (1999)*
Maximum Aquifer Thickness	Maximum depth from land surface to aquifer bottom	
Bay Slope Max (percent rise)	Steepest slope in the Bay	*Moore et al. (1993); McKenzie and Ryan (1999); Venteris et al. (2004); Thompson et al. (2006); Schwanghart and Jarmer (2011); Pastick et al. (2014)*
Total Curvature: - **Upslope Average** - **Bay Maximum**	Combination of horizontal and vertical curvature	See Table 14
Planar Curvature: - **Upslope Maximum** - **Bay Average**	Horizontal curvature	
Profile Curvature: - **Upslope Average**	Vertical curvature	
Tangential Curvature: - **Upslope Maximum** - **Bay Minimum**	Measure of local flow convergence (planar curvature times slope gradient)	
TCI Average	Average soil transport capacity of upslope area	*Thompson et al. (2006)*
Upslope Flow Path Length Max	Maximum flowpath for surface water in the upslope catchment area	*Moore et al. (1993); Venteris et al. (2004); Thompson et al. (2006); Schwanghart and Jarmer (2011)*
Ditch Depth Average	Average depth of ditches running through Bays	
Known Drainage	Presence or absence of obvious evidence of anthropogenic drainage in the Bay (e.g., ditches, covered grates leading to underground pipes)	

Table 11. *Previous soil–landscape studies that have used curvature as topographic attributes and the types of curvature examined.*

Moore et al. (1993)	McKenzie and Ryan (1999)	Venteris et al. (2004)	Thompson et al. (2006)	Schwanghart and Jarmer (2011)
Profile	Profile	Profile	Profile	Profile
Planar	Planar	Planar	Planar	Planar
	Tangential	Cross sectional	Tangential	
		Longitudinal	Total	
		Maximum, minimum, and mean in any plane		

According to Smedema et al. (2004) in their handbook/textbook on modern land drainage, good drainage engineering and management requires attention to subsurface hydrology and topography. Moderate to high correlation was found between SOC stock and known drainage ($r = 0.495$) and SOC and average ditch depth ($r = 0.736$). That either variable could achieve a correlation coefficient greater than 0.3 given the very low correlations of most of the other variables to SOC stock may be significant. One possibility could be that deeper average ditch depth and the obvious presence of anthropogenic drainage systems are linked to wetter Bays due, in part, to the Bay basin being closer to the top of the surficial aquifer. Alternatively, the relatively strong correlations to SOC stock may be artifacts of the small sample size (7 Bays with known drainage and 4 Bays with ditches). Drainage of these Bays may not have been explicitly planned or designed with regards to topography or subsurface water as advocated by Smedema et al. (2004).

3.3.3 Carbon–Terrain Analysis

GLM, GAM, and PLSR models were run using 16, 11, and 7 variables (Table 12). GLM and PLSR were also run using all of the original variables, but GAM was unable to handle 50 variables for only 28 observations. All data collected for this study was input into building the five models. Despite running leave-one-out cross validation, high R^2 values are used as an

indication of potential predictive power or accuracy. While comparison of model performance in this section is based on R^2, there has been no outside validation using additional data.

GLM with ridge regularization greatly out performed LASSO. While LASSO did return R^2 values greater than ridge, examination of the selected variables using LASSO showed only variables relating to ditches were used, making this model useless for Bays lacking ditches. Ridge regularization of GLM forced the model to assign values to all variables making this model more accurate and useful. GLM ridge performance is negatively impacted by collinear variables, but a CI threshold of 30 is sufficient to return fairly strong prediction accuracy. Due to the nature of the terrain attributes, i.e., overall weak correlation to SOC stock, as few variables should be removed as possible. A low CI threshold of 10 begins to decrease model fit by removing too many variables when compared with a CI threshold of 30.

Table 12. *Statistics for GLM, GAM, and PLSR predictive models of SOC stock. The number of variables that produced the best goodness of fit (R^2) for each model is italicized.*

GLM, LASSO				**GLM, Ridge**			
Variables	Percent Deviance	R^2	RMSE	Variables	Percent Deviance	R^2	RMSE
7	0.378	0.378	7.4	**7**	0.402	0.402	6.7
11	0.378	0.378	7.4	***11***	*0.599*	*0.599*	*6.4*
16	0.439	0.439	7.2	**16**	0.015	0.154	7.7
All	*0.499*	*0.499*	*6.9*	**All**	0.031	0.221	7.2

GAM Models					
Variables	Non-penalized		Variables	Cubic Splice	
	R^2	RMSE		R^2	RMSE
7	0.674	4.6	**7**	0.632	6.0
11	0.784	7.6	***11***	*0.679*	*6.6*
16	*0.882*	*4.9*	**16**	0.434	7.8

PLSR					
Variables	Components	Min. PRESS Statistic	RMSEP	R^2	RMSE
7	2	51712.1	42.9	0.005	8.4
11	2	40458.9	38.0	0.202	7.7
16	2	45744.6	40.4	0.326	5.8
All	*2*	*45445.4*	*40.3*	*0.370*	*5.3*

Unlike the other models PLSR does not look at the relationship between the independent and dependent variables, but acts in a manner more like principal component analysis (PCA). Contrary to the prediction of Dormann et al. (2013) regarding variables with weaker correlation the use of a latent variable method (PLSR) did not out perform penalization and variable selection. Although PLSR can be used for analyses involving many variables and highly collinear data, the poor performance of this model compared to GLM and GAM suggest it is not appropriate for modeling or predicting spatial variation of soil in the study area.

Despite an inability to handle all of the variables, the GAM models performed the best based on R^2 and RMSE values. The relatively small changes in R^2 and RMSE between 16, 11, and 7 included variables for both the un-penalized and cubic spliced GAM suggests a greater resilience to collinear variables than the GLM. Despite the use of leave-one-out cross-validation a second independent dataset is suggested to assess overfitting of the un-penalized GAM. Such an assessment was beyond the scope of this study. Therefore, cubic splice GAM using variables with a maximum CI threshold of 30 is considered the best of these models. The ability of GAM and GLM using ridge regularization to generate models with R^2 values greater than 0.5 demonstrates that the idea in Thompson et al. (2006) and Venteris et al. (2004) regarding the applicability of non-linear models for soil–landscape modeling works for low relief landscapes.

While a large number of terrain attributes were examined in this study, a number of factors were unable to be incorporated. As briefly discussed in the previous chapter, land use can impact SOC levels but changes in soil carbon—whether increasing or decreasing—occurs over time. Three potentially significant unexplored variables are tied to land use: time since conversion, type of crop(s) cultivated on the sites, and land management/agricultural practices (e.g., fertilization, tillage, crop rotation). A fourth important variable for consideration is the

initial SOC stock prior to conversion. All four of these factors contribute to the rate of change in SOC and potentially could drastically increase model prediction accuracy (Goidts and van Wesemael, 2007). Unfortunately, such data are difficult, if not impossible, to obtain.

3.4 Conclusion

SOC stock varies widely among prior converted Delmarva Bays ranging from 49.5 Mg/ha to 219.2 Mg/ha with a mean around 93 Mg/ha. In keeping with previous work in this area a weak relationship was found between terrain attributes and soil carbon. By using a number of the attributes together, moderately accurate predictive models ($R^2 \geq 0.5$) were created based solely on topography. The wide range of results among the five models examined show (1) non-linear modeling can be used to predict soil carbon distribution in low relief landscapes, and (2) the choice of model and CI threshold can greatly affect prediction accuracy. While a large number of terrain attributes were examined in this study they do not encompass all topographic factors. The inclusion of variables pertaining to land use and land use history in particular may increase topography based prediction models of soil carbon in the study area.

4 Effects of Analytic Strategies and Soil Condition on Spectral-based Predictions of Soil Organic Carbon Among Agriculturally Converted Delmarva Bays

4.1 Introduction

Hypersectral soil data analysis in the lab is almost always performed on dried and powder ground samples to get an idealized 'pure' spectral signature devoid of influence from moisture and non uniform texture. While such data do have uses, research based on dry ground soil provides little guidance for using spectroscopy under field conditions. Studies such as McCarty et al. (2010) reveal predictive accuracy of hyperspectral models can change when data is recorded in the field versus in the lab. Mid-infrared data is more robust to changes between field and lab soil spectra than the near-infrared and visible regions, but mid-infrared is less accessible.

Chang et al. (2005) found soil moisture has little impact on prediction accuracy of soil carbon despite drastically changing the appearance of a soil's spectra. However, the moist samples were ground before hyperspectral readings were taken so the combined effect of moisture on unground samples remains in questions. Additionally, the soil Chang et al. (2005) studied had much lower soil moisture content than would likely be encountered in a wetland which might affect model performance.

Spectral data has been and is increasingly used to study soil properties and wetlands, yet literature implementing spectroscopy in the study of wetland soil remains almost non-existent. Of these studies, none could be found in which the hyperspectral soil data was collected on un-dried and/or unground samples. This study examines the relationship of hyperspectral data to carbon concentration in prior converted Delmarva Bays. The goals of this study is to assess how applicable point spectroscopy is for studying wetland soil properties by (1) evaluating prediction accuracy of hyperspectral data using four smoothing techniques on moist unground, air dried

unground, and air dried ground soil samples; and (2) examining the effect of moisture and non uniform particle size on hyperspectral estimates of soil carbon.

4.2 Methods

4.2.1 Spectroscopy

Spectral signatures for all first horizons were taken in the lab using an ASD FieldSpec 3, which records 350 nm to 2500 nm with sampling intervals of 1.4 nm from wavelengths 350 nm to 1000 nm and 2 nm for 1000 nm to 2500 nm. The spectroradiometer was set to take and average 10 readings every second. All readings taken used a contact probe and the instrument was recalibrated after each reading using Spectralon for the white reference. Although the ASD FieldSpec was used in a lab setting, this equipment and method for recording the spectral signatures can be used in the field. Spectroscopy was carried out on a subset—the topmost soil horizons—of the soil samples collected in the previous chapter.

Spectral profiles for all 84 first horizons were collected after the samples had been air dried, ground, and passed through a 2 mm sieve, in preparation for the carbon analysis. The spectral profile for each sample was taken four times from different locations in the sample and averaged following the method described by Cohen et al. (2005). For 18 of these samples, spectral signatures were taken two additional times: when the samples were moist, and when the samples were dry and unground. The percent of water present in the moist samples was calculated using the difference in weight between before and after the samples were air-dried (Table 13). Sampled during winter, several Bays were becoming inundated with water puddling at the surface during field data collection due to a rising water table and frequent rainfall (Figure 5).

Figure 5. *Puddling of water in one of the sampled Bays during fieldwork.*

Table 13. *Percent of water present in the samples of the moist dataset.*

Wet Weight (g)	Dry Weight (g)	Percent Water
407.9	282.7	30.7
317.3	267.2	15.8
352.9	252.4	28.5
367.5	296.7	19.3
320	235.3	26.5
360.9	271.0	24.9
348.8	258.9	25.8
286.4	237.9	16.9
266.7	214.9	19.4
291.3	239.1	17.9
310.3	265.8	14.4
307.5	233.3	24.2
334.6	246.4	26.4
268.6	215.4	19.8
335.9	258.9	22.9
337.5	255.2	24.4
309.1	254.8	17.6
302.9	249.4	17.7
Minimum		14.4
Maximum		30.7
Mean		21.8

4.2.2 Statistical Analysis

After it was determined no large steps were present in any of the data, spectral data were transformed into reflectance and splice correction carried out to interpolate data for small jumps using ViewSpec Pro. Reflectance data were exported from ViewSpec Pro into RStudio 3.3.1 for

processing and analysis. Following Hively et al. (2011) and Stein et al. (2014) a number of math pretreatments were used to compare which was best suited for the task, namely capturing slight variations in SOC concentration of the topmost soil horizon: reflectance (R), log (1/R), first derivative, and second derivative. Logarithmic transformation of reflectance data into absorption is common practice in hyperspectral studies (Steine et al., 2014). First and second derivatives magnify features and are also frequently used with spectral data. Based on the partial least squares regression (PLSR) goodness of fit (R^2) results associated with soil carbon in Hively et al. (2011) 2 gap and 4 gap first derivatives and 16 gap and 4 gap second derivatives were used. In Hively et al. (2011) these gaps produced the two highest R^2 values for the first and second derivatives for predicting soil carbon in agricultural fields situated within the Upper Choptank watershed.

As smoothing can remove information as well as noise, and as there are a wide number of smoothing techniques (Vaiphasa 2006), the SOC predictive capacity of unsmoothed data were compared with mean centered and second order Savitzky-Golay filtering. In order to make the Savitzky-Golay filtering comparative to previous work on wetland soils (i.e., Cohen et al., 2005; Cohen et al., 2007) and previous work done on soils in the study area (i.e., Hively et al., 2011), this smoothing was applied and analyzed twice: on the original reflectance data using a 20 nm gap, and on reflectance data resampled to 10 nm resolution and using a 20 nm gap. PLSR analysis with leave-one-out cross-validation was run to generate predictive models for all math pretreatments and smoothing transformations. The number of factors chosen for the PLSR was determined using the minimum root mean PRESS statistic (McCarty et al., 2002; Hively et al., 2011). The best model for each smoothing model was selected based on the smallest minimum PRESS statistic for the three dataset—moist unground, air dried unground, and air dried ground

soil samples. Performance of models using these three datasets were compared using goodness of fit (R^2) and root mean square error (RMSE) as calculated in chapter two.

Although the majority of soil carbon contained in non Spodosols is usually found in the top horizon and hyperspectral data can provide accurate predictions on carbon concentration of individual horizons, variation in top horizon carbon concentration between locations does not necessarily correspond with variation in carbon stock of the first meter. A linear model was run to assess the relationship between 1 m carbon stock and carbon concentration of the top soil horizon.

4.3 Results and Discussion

Using the six selected math treatments, almost all smoothing techniques returned R^2 values greater than 0.9 for the model with the minimum PRESS (Table 14). Three exceptions are both versions of the Savitzky-Golay filter when performed on dry unground samples, and the resampled Savitzky-Golay filter when run on the moist unground samples. All spectral data collected for this study went into building the models. No validation of actual model performance was run using additional data. R^2 analysis, which was validated using leave-one-out cross validation, is assumed to represent potential model performance based solely on the training data. Verification of these models with a separate dataset may reveal a disconnect between internal R^2 values and actual performance.

In general, reflectance and log math treatments return the best models, although all datasets had derivatives return the best models when the resampled Savitzky-Golay filter was used. Dry ground sample models use more components than the other two datasets and return higher minimum PRESS statistics. However, the higher numbers of components and minimum PRESS statistics for dry unground soil is expected given that a much higher number of samples

Table 14. *Effects of math treatments and smoothing on SOC stock predictions of dry ground, dry unground, and moist unground samples. The math treatment of each smoothing technique resulting in the smallest minimum PRESS is italicized for each dataset.*

	No Smoothing						
	Math Treatment	Components	Min PRESS Statistic	RMSEP	% Variance Explained	R^2	RMSE
Dry Ground Samples	***Reflectance***	*16*	*8.51*	*0.318*	*100*	*0.925*	*0.134*
	Log	18	8.79	0.324	100	0.961	0.097
	1st Derivative, 2 gap	3	11.39	0.368	64.0	0.710	0.264
	1st Derivative, 4 gap	4	9.59	0.338	83.7	0.736	0.252
	2nd Derivative, 4 gap	1	14.69	0.419	12.9	0.406	0.378
	2nd Derivative, 16 gap	7	8.85	0.325	91.4	0.811	0.213
Dry Unground Samples	**Reflectance**	6	1.31	0.270	99.9	0.788	0.151
	Log	*9*	*0.81*	*0.212*	*99.9*	*0.983*	*0.043*
	1st Derivative, 2 gap	1	2.18	0.348	14.8	0.528	0.225
	1st Derivative, 4 gap	1	2.05	0.337	26.2	0.310	0.272
	2nd Derivative, 4 gap	1	2.36	0.362	15.9	0.473	0.238
	2nd Derivative, 16 gap	1	1.96	0.330	33.8	0.227	0.288
Moist Unground Samples	***Reflectance***	*14*	*1.23*	*0.261*	*100*	*0.999*	*0.004*
	Log	1	1.69	0.306	69.9	0.199	0.293
	1st Derivative, 2 gap	9	1.24	0.262	94.9	0.999	0.006
	1st Derivative, 4 gap	7	1.65	0.302	97.9	0.987	0.038
	2nd Derivative, 4 gap	6	1.31	0.270	78.5	0.998	0.016
	2nd Derivative, 16 gap	4	1.42	0.281	95.2	0.757	0.162

	Mean Centering						
	Math Treatment	Components	Min PRESS Statistic	RMSEP	% Variance Explained	R^2	RMSE
Dry Ground Samples	**Reflectance**	14	8.46	0.317	99.9	0.908	0.149
	Log	*16*	*8.23*	*0.313*	*100*	*0.939*	*0.121*
	1st Derivative, 2 gap	3	12.39	0.385	48.4	0.685	0.275
	1st Derivative, 4 gap	5	9.99	0.345	79.2	0.765	0.237
	2nd Derivative, 4 gap	1	15.39	0.429	11.9	0.369	0.389
	2nd Derivative, 16 gap	8	8.74	0.323	92.1	0.832	0.201
Dry Unground Samples	**Reflectance**	5	1.34	0.273	99.9	0.734	0.169
	Log	*9*	*0.82*	*0.327*	*99.9*	*0.928*	*0.088*
	1st Derivative, 2 gap	1	2.32	0.359	13.5	0.559	0.218
	1st Derivative, 4 gap	2	2.32	0.359	54.2	0.563	0.217
	2nd Derivative, 4 gap	1	2.61	0.380	20.0	0.350	0.264
	2nd Derivative, 16 gap	1	2.06	0.339	20.3	0.327	0.269
Moist Unground Samples	**Reflectance**	12	1.53	0.292	99.9	0.997	0.019
	Log	1	1.70	0.317	72.2	0.191	0.294
	1st Derivative, 2 gap	*6*	*1.12*	*0.249*	*81.8*	*0.998*	*0.015*
	1st Derivative, 4 gap	7	1.29	0.268	95.7	0.994	0.025
	2nd Derivative, 4 gap	8	1.15	0.252	70.7	0.999	0.010
	2nd Derivative, 16 gap	6	1.13	0.250	98.1	0.927	0.089

	Savitzky-Golay Filtering, 21nm window						
	Math Treatment	Components	Min PRESS Statistic	RMSEP	% Variance Explained	R^2	RMSE
Dry Ground Samples	***Reflectance***	*18*	*7.89*	*0.307*	*100*	*0.912*	*0.146*
	Log	15	8.59	0.319	100	0.88	0.170
	1st Derivative, 2 gap	4	9.03	0.328	89.3	0.708	0.265
	1st Derivative, 4 gap	4	8.99	0.327	90.1	0.703	0.267
	2nd Derivative, 4 gap	4	10.59	0.356	61.9	0.766	0.237
	2nd Derivative, 16 gap	7	8.52	0.319	92.2	0.804	0.217
Dry Unground Samples	**Reflectance**	6	1.24	0.262	99.9	0.800	0.146
	Log	*5*	*1.17*	*0.255*	*99.9*	*0.762*	*0.159*
	1st Derivative, 2 gap	2	1.88	0.324	68.3	0.373	0.259
	1st Derivative, 4 gap	2	1.86	0.321	69.9	0.363	0.261
	2nd Derivative, 4 gap	1	2.25	0.353	15.9	0.474	0.238
	2nd Derivative, 16 gap	1	1.99	0.333	36.3	0.199	0.293
Moist Unground Samples	***Reflectance***	*12*	*1.31*	*0.270*	*100*	*0.982*	*0.045*
	Log	1	1.69	0.307	72.2	0.191	0.294
	1st Derivative, 2 gap	4	1.57	0.296	97.0	0.646	0.195
	1st Derivative, 4 gap	4	1.57	0.295	97.4	0.610	0.204
	2nd Derivative, 4 gap	1	1.62	0.299	42.9	0.251	0.283
	2nd Derivative, 16 gap	4	1.38	0.277	97.8	0.669	0.188

	Savitzky-Golay Filtering, 21nm window – 10nm re-sampled data						
	Math Treatment	Components	Min PRESS Statistic	RMSEP	% Variance Explained	R^2	RMSE
Dry Ground Samples	**Reflectance**	22	7.43	0.298	100	0.888	0.164
	Log	26	6.47	0.278	100	0.925	0.134
	1st Derivative, 2 gap	*25*	*6.18*	*0.271*	*100*	*0.934*	*0.126*
	1st Derivative, 4 gap	29	6.91	0.287	100	0.933	0.127
	2nd Derivative, 4 gap	11	8.69	0.322	99.4	0.792	0.224
	2nd Derivative, 16 gap	8	8.70	0.322	99.5	0.703	0.267
Dry Unground Samples	**Reflectance**	8	1.22	0.26	100	0.866	0.119
	Log	7	1.24	0.263	99.9	0.796	0.148
	1st Derivative, 2 gap	*7*	*1.04*	*0.241*	*99.9*	*0.807*	*0.144*
	1st Derivative, 4 gap	8	1.35	0.274	99.7	0.887	0.110
	2nd Derivative, 4 gap	4	1.93	0.328	94.2	0.660	0.191
	2nd Derivative, 16 gap	2	1.92	0.327	90.3	0.116	0.308
Moist Unground Samples	**Reflectance**	1	1.73	0.309	92.1	0.142	0.303
	Log	1	1.71	0.308	81.3	0.171	0.298
	1st Derivative, 2 gap	1	1.73	0.321	97.6	0.142	0.303
	1st Derivative, 4 gap	3	1.49	0.288	96.6	0.561	0.217
	2nd Derivative, 4 gap	4	1.48	0.287	99.6	0.643	0.196
	2nd Derivative, 16 gap	*3*	*1.47*	*0.286*	*99.3*	*0.465*	*0.239*

went into creating this dataset, 84 versus 18. Components and PRESS statistics may be lowered if the minimum PRESS model is used as a starting point and selection of the optimum model is

based on t-tests run between the RMSE of the minimum PRESS model and the RMSE of the lower component models (Rossel et al., 2006).

From comparison of the best models, those based on moist unground samples returned the highest R^2 for all smoothing techniques except for the resampled Savitzky-Golay filter. The ability of PLSR to produce high-accuracy predictive models from moist samples, as reported by Change et al. (2005) when analyzing moist ground samples, was reaffirmed using samples with much higher soil moisture content. Based on results of the current study the influence of soil texture on predictive accuracy appears to be masked by effects of water when moisture is present in the samples. The findings of this study also support the work of Cohen et al. (2005) and Cohen et al. (2007) in their conclusion that hyperspectral data forms a viable means for studying spatial distributions of wetland soil properties. However, the poor performance of the resampled Savitzky-Golay filter method on the moist unground data argues against use of this smoothing technique for *in situ* data collection of carbon data within wetland soils.

The various smoothing techniques examined here can return strong predictive models of soil carbon, but they are dependent on analytical strategies and the degree of soil processing (drying and grinding). High-accuracy prediction models using data collected from soil samples with non-uniform texture and high moisture levels demonstrate the potential for point spectroscopy as a useful and nondestructive way to study the spatial distribution of soil carbon. However, the choice of math treatment and smoothing technique used for point spectroscopy should not be selected *ad hoc* based on performance of air-dried ground lab samples. The results of this study support the use of a quantitative approach to selecting smoothing methods as advocated by Vaiphasa (2006) run on either *in situ* field sampling data or lab hyperspectral data of unprocessed samples (e.g., unground and not dried).

The linear regression between the carbon stock and top layer carbon concentration showed a very strong relationship at a 95% confidence interval. Despite the strong relationship, top layer carbon concentration only accounted for half ($R^2 = 0.493$) of the variation seen in carbon stock within the upper first meter. While most top soil layers contained the highest concentrations of carbon, some of the wetlands examined in this study have their highest carbon concentrations below the surface. Therefore, it is important to remember hyperspectral data can only provide estimates of SOC concentration in the soil layer it is reading. Hyperspectral estimates of the spatial distribution of top layer soil carbon should not be interpreted as necessarily representing absolute variation in soil carbon stock, rather they can serve as a starting point or an additional input of data to strengthen predictive models.

4.4 Conclusion

Effects of smoothing on hyperspectral soil data are highly variable with multiple techniques having little impact on predictive models and others severely influencing the outcome. The physical state of soil samples, i.e., ground versus unground and moist/wet versus dry, effects the math treatment and smoothing technique best suited for the study area when selection is based on minimum PRESS statistic. Due to the overall high R^2 for the predictive models of near-infrared and visible hyperspectral data of moist unground soil samples point spectroscopy is a viable and non-destructive method for studying carbon, and potentially other soil properties, in wetland soils. Despite the success of Cohen et al. (2005) and Cohen et al. (2007) in predicting soil carbon using the resampled Savitzky-Golay filter on dried ground samples, this technique is not advised for data collected from moist unground samples. As the dried ground dataset proved the most robust in terms of the R^2, selection of smoothing and math

treatment for hyperspectral data collected *in situ* should not be chosen based on what has previously worked well when using processed soil samples.

5 Conclusions

SOC stocks found in prior converted Delmarva Bays can vary widely, from 50 to 218 Mg/ha. Individual terrain attributes tend to have weak correlation with Bay carbon stock, but topography can account for a significant portion of soil carbon distribution as assessed by non-linear models. GAM and GLM using ridge regularization return moderately strong topographic-based predictive models of Bay carbon stock ($R^2 \geq 0.5$). Model strength was highest when variables had a CI lower than 30 and greater than 10. The decrease in potential model performance with the lower CI threshold is likely a result of the overall weak relationship between individual terrain attributes and SOC. Performance of GAM and GLM ridge Bay SOC models may increase with the additional input of hyperspectral soil data. Hyperspectral data of the visible and near-infrared can provide highly accurate predictions ($R^2 \geq 0.9$) of Bay SOC concentration regardless of soil moisture or texture uniformity. However, both Savitzy-Golay smoothing techniques had little effect on the dried ground sample model and decreased model accuracy of the dried unground and moist unground samples.

A large number of terrain attributes, 50 in all, were examined with regards to Bay SOC stock, but they are not an exhaustive list of how topography may influence soil carbon distribution. It was beyond the scope of this study to examine effects of four specific topographic factors that may strongly impact SOC stock: time since conversion, choice of crop(s) cultivated on the sites, land management/agricultural practices, and initial SOC stock before agricultural conversion.

Non-linear topography-based models can provide a means for predicting the spatial distribution of soil properties. When dealing with low relief landscapes where linear models have been previously unsuccessful and data is highly collinear the model type is very important.

While GLM is the more commonly known non-linear alternative for modeling soil–landscape interaction, GAM can perform very well, although caution should be applied concerning the latter's tendency to overfit data.

PLSR generates a poor topography-based predictive model of soil carbon, but can create strong predictive models using hyperspectral data of near-infrared and visible wavelengths. While hyperspectral data can predict soil carbon concentration distribution horizontally across the top soil horizon, surface variation should not be assumed to represent variation of soil property stock (mass). Based on results of moist unground soil samples, *in situ* hyperspectral data collection could provide accurate predictions of relative soil carbon, and potentially other soil properties', distribution. However, when deciding on how to process hyperspectral data collected in the field, experimentation may be necessary to select the best method for the soil property under examination.

References

Anne, N.J.P., A.H. Abd-Elrahman, D.B. Lewis, and N.A. Hewitt. 2014. Modeling soil parameters using hyperspectral image reflectance in subtropical coastal wetlands. Int. J. Appl. Earth Obs. Geoinf. 33: 47-56.

Bartholomeus, H.M., M.E. Schaepman, L. Kooistra, A. Stevens, W.B. Hoogmoed, and O.S.P. Spaargaren. 2008. Spectral reflectance based indices for soil organic carbon quantification. Geoderma 145: 28-36.

Batjes, N.H. 1996. The total C and N in soils of the world. Soil Science 47:151-163.

Bedard-Haughn, A., F. Jongbloed, J. Akkerman, A. Uijl, E. de Jong, T. Yates, and D. Pennock. 2006. The effects of erosional and management history on soil organic carbon stores in ephemeral wetlands of hummocky agricultural landscapes. Geoderma 135: 296-306.

Bohn, T.J., E. Podest, R. Schroeder, N. Pinto, K.C. McDonald, M. Glagolev, I. Filippov, S. Maksyutov, M. Heimann, X. Chen, and D.P. Lettenmaier. 2013. Modeling the large-scale effects of surface moisture heterogeneity on wetland carbon fluxes in the West Siberian Lowland. Biogeosciences 10: 6559–6576.

Bouchard, V., D. Gillon, R. Joffre, and J.C. Lefeuvre. 2003. Actual litter decomposition rates in salt marshes measured using near-infrared reflectance spectroscopy. J. Exp. Mar. Biol. Ecol. 290: 149–163.

Bridgham, S.D., J.P. Megonigal, J.K. Keller, N.B. Bliss, and C. Trettin. 2006. The Carbon Balance of North American Wetlands. Wetlands 26(4): 889–916.

Brinson, M.M. 1993. A hydrogeomorphic classification of wetlands. Technical Report WRP-DE-4, U.S. Army Engineer Waterways Experiment Station, Vicksburg, MS.

Brinson, M.M., and S.D. Eckles. 2011. U.S. Department of Agriculture Conservation Program and Practice Effects on Wetland Ecosystem Services: A Synthesis. Ecol. Appl. 2: S116–27.

Bruce, J.P., M. Frome, E. Haites, H. Janzen, R. Lal, and K. Paustian. 1999. Carbon sequestration in soils. J. Soil Water Conserv. 54: 382–389.

Chang, C.W., D.A. Laird, and C.R. Hurburgh. 2005. Influence of Soil Moisture on Near-Infrared Reflectance Spectroscopic Measurement of Soil Properties. Soil Science 170(4): 244–255.

Cohen, M.J., J.P. Prenger, and W.F. DeBusk. 2005. Visible-Near Infrared Reflectance Spectroscopy for Rapid, Nondestructive Assessment of Wetland Soil Quality. J. Environ. Qual. 34: 1422–1434.

Cohen, M.J., J. Paris, and M.W. Clark. 2007. P-sorption Capacity Estimation in Southeastern USA Wetland Soils Using Visible/Near Infrared (VNIR) Reflectance Spectroscopy. Wetlands 27(4): 1098–1111.

Craft, C.B., and W.P. Casey. 2000. Sediment and Nutrient Accumulation in Floodplain and Depressional Freshwater Wetlands of Georgia, USA. Wetlands 20(2): 323-332.

Croft, H., N.J. Kuhn, and K. Anderson. 2012. On the use of remote sensing techniques for monitoring spatio-temporal soil organic carbon dynamics in agricultural systems. Catena 94: 64-74.

Dalal, R., and S. Shanmugam. 2015. Consulting Study 6: Practical guidance on how to estimate soil carbon stocks and soil greenhouse gas emissions following tropical forest conversion on mineral soil. High Carbon Stock Science Study.

Denver, J.M., and M.R. Nardi. 2015. Thickness of the Surficial Aquifer, Delmarva Peninsula,

Maryland and Delaware. Raster Digital Data Set. Digital Data Series 99999. USGS, Reston, VA.
Dormann, C.F., J. Elith, S. Bacher, C. Buchmann, G. Carl, G. Carré, J.R. García Marquéz, B. Gruber, B. Lafourcade, P.J. Leitā, T. Münkemüller, C. McClean, P.E. Osborne, B. Reineking, B. Schröder, A.K. Skidmore, D. Zurell, and S. Lautenbach. 2013. Collinearity: a review of methods to deal with it and a simulation study evaluating their performance. Ecography 36: 27–46.
Eckles, S.D. 2011. Linking Science, Policy and Management to Conserve Wetlands in Agricultural Landscapes. Ecol. Appl. 21: S1–2.
Fenstermacher, D. E. 2011. Carbon Storage and Potential Carbon Sequestration in Depressional Wetlands of the Mid-Atlantic Region. Master of Science, College Park, Maryland: University of Maryland.
Fenstermacher, D.E., M.C. Rabenhorst, M.W. Lang, G.W. McCarty, and B.A. Needelman. 2014. Distribution, Morphometry, and Land Use of Delmarva Bays. Wetlands 34(6): 1219–1228.
Gomez, C., R.A.V. Rossel, A.B. McBratney. 2008. Soil organic carbon prediction by hyperspectral remote sensing and field vis-NIR spectroscopy: An Australian case study. Geoderma 146: 403-411.
Goidts, E., and B. van Wesemael. 2007. Regional assessment of soil organic carbon changes under agriculture in Southern Belgium (1955–2005). Geoderma 141: 341–354.
Hively, W.D., G.W. McCarty, J.B. Reeves III, M.W. Lang, R.A. Oesterling, and S.R. Delwiche. 2011. Use of Airborne Hyperspectral Imagery to Map Soil Properties in Tilled Agricultural Fields. Applied and Environmental Soil Science 2011: 1–13.
Edenhofer, O., R. Pichs-Madruga, Y. Sokona, E. Farahani, S. Kadner, K. Seyboth, A. Adler, I. Baum, S. Brunner, P. Eickemeier, B. Kriemann, J. Savolainen, S. Schlömer, C. von Stechow, T. Zwickel and J.C. Minx (ed.). 2014. Climate Change 2014: Mitigation of Climate Change. Contribution of Working Group III to the Fifth Assessment Report of the Intergovernmental Panel on Climate Change. IPCC, Cambridge University Press, Cambridge, UK.
Ju, W., and J.M. Chen. 2005. Distribution of soil carbon stocks in Canada's forests and wetlands simulated based on drainage class, topography and remotely sensed vegetation parameters. Hydrol. Process. 19: 77–94.
Luo, Y., and X. Zhou. 2006. Soil respiration and the environment. Elsevier, Inc, Burlington, MA.
Maryland Department of Natural Resources. 2005. Characterization Of The Upper Chester River Watershed In Kent County and Queen Anne's County, Maryland. Maryland Department of Natural Resources. DNR-14-1209-0022.
McCarty, G.W., J.B. Reeves III, V.B. Reeves, R.F. Follett, and J.M. Kimble. 2002. Mid-infrared and Near-Infrared Diffuse Reflectance Spectroscopy for Soil Carbon Measurement. Soil Sci. Soc. Am. J. 66: 640–646.
McCarty, G.W., and J.B. Reeves III. 2006. Comparison of near infrared and mid infrared diffuse reflectance spectroscopy for field-scale measurements of soil fertility parameters. Soil Science 171(2): 94–102.
McCarty, G.W., L.L. McConnell, C.J. Hapeman, A. Sadeghi, C. Graff, W.D. Hively, M.W. Lang, T.R. Fisher, T. Jordan, C.P. Rice, E.E. Codling, D. Whitall, A. Lynn, J. Keppler, and M.L. Fogel. 2008. Water quality and conservation practice effects in the Choptank River watershed. J. Soil Water Conserv. 63(6): 461–474.

McDonough, O.T., M. Lang, J.D. Hosen, and M.A. Palmer. 2015. Surface Hydrologic Connectivity Between Delmarva Bay Wetlands and Nearby Streams Along a Gradient of Agricultural Alteration. Wetlands 35(1): 41–53.
McKenzie, N.J., and P.J. Ryan. 1999. Spatial prediction of soil properties using environmental correlation. Geoderma 89: 67–94.
Millennium Ecosystem Assessment. 2005. Ecosystems and Human Well-Being: Wetlands and Water. World Resources Institute, Washington, D.C.
Moore, I.D., P.E. Gessler, G.A. Nielsen, and G.A. Peterson. 1993. Soil Attribute Prediction Using Terrain Analysis. Soil Sci. Soc. Am. J. 57: 443–452.
Morse, J.L., M. Ardón, and E.S. Bernhardt. 2012. Greenhouse Gas Fluxes in Southeastern U.S. Coastal Plain Wetlands under Contrasting Land Uses. Ecol. Appl. 22(1): 264–80.
Murty, D., M.F. Kirschbaum, R.E. McMurtrie, and H. McGilvray. 2002. Does Conservation of Forest to Agricultural Land Change Soil Carbon and Nitrogen? A Review of the Literature. Global Change Biol. 8: 105–23.
Pastick, N.J., M. Rigge, B.K. Wylie, M.T. Jorgenson, J.R. Rose, K.D. Johnson, and L. Ji. 2014. Distribution and landscape controls of organic layer thickness and carbon within the Alaskan Yukon River Basin. Geoderma 230: 79–94.
Reese, R.E., and K.K. Moorhead. 1996. Spatial Characteristics of Soil Properties along an Elevational Gradient in a Carolina Bay Wetland. Soil Sci. Soc. Am. J. 60: 1273–1277.
Rivero, R.G., S. Grunwald, and G.L. Bruland. 2007. Incorporation of spectral data into multivariate geostatistical models to map soil phosphorous variability in a Florida wetland. Geoderma 140: 428–443.
Rossel, R.A.V., D.J.J. Walvoort, A.B. McBratney, L.J. Janik, and J.O. Skjemstad. 2006. Visible, near infrared, mid infrared or combined diffuse reflectance spectroscopy for simultaneous assessment of various soil properties. Geoderma 131: 59–75.
Schwanghart, W., and T. Jarmer. 2011. Linking spatial patterns of soil organic carbon to topography – A case study from south-eastern Spain. Geomorphology 126: 252–263.
Sequeira, C.H., S.A. Wills, C.A. Seybold, and L.T. West. 2014. Predicting soil bulk density for incomplete databases. Papers in Natural Resources. Paper 397.
Smedema, L.K., W.F. Vlotman, and D. Rycroft. 2004. Modern Land Drainage: Planning, Design and Management of Agricultural Drainage Systems. A.A. Balkema Publishers, Taylor & Francis Group. London, UK.
Stein, B.R., V.A. Thomas, L.J. Lorentz, and B.D. Strahm. 2014. Predicting macronutrient concentrations from loblolly pine leaf reflectance across local and regional scales. GIScience & Remote Sensing 51(3): 269–287.
Stolt, M.H., and M.C. Rabenhorst. 1987. Carolina Bays on the Eastern Shore of Maryland: I. Soil Characterization and Classification. Soil Sci. Soc. Am. J. 51 (2): 394–98.
Stolt, M.H., M.H. Genthner, W.L. Daniels, and V.A. Groover. 2001. Spatial Variability in Palustrine Wetlands. Soil Sci. Soc. Am. J. 65: 527-535.
Suchenwirth, L., M. Förster, A. Cierjacks, F. Lang, and B. Kleinschmit. 2012. Knowledge-based classification of remote sensing data for the estimation of below- and above-ground organic carbon stocks in riparian forests. Wetlands Ecol. Manage. 20: 151-163.
Thompson, J.A., E.M. Pena-Yewtukhiw, and J.H. Grove. 2006. Soil—landscape modeling across a physiographic region: Topographic patterns and model transportability. Geoderma 133: 57–70.
Tiner, R.W., H.C. Bergquist, G.P. DeAlessio, and M.J. Starr. 2002. Geographically Isolated

Wetlands: A Preliminary Assessment of Their Characteristics and Status in Selected Areas of the United States. U.S. Department of the Interior, Fish and Wildlife Services, Northeast Region, Hadley, MA.
Tiner, R.W. 2015. Wetlands: An Overview. p. 3–18. *In* M. Lang et al. (ed.). Remote Sensing of Wetlands: Applications and Advances. CRC Press, Taylor & Francis Group. Boca Raton, FL.
U.S. Army Corps of Engineers. 2010. Regional Supplement to the Corps of Engineers Wetland Delineation Manual: Atlantic and Gulf Coastal Plan Region (version 2.0). U.S. Corps of Engineers. Vicksburg, MS.
USDA Natural Resources Conservation Service. 2010. Nation Food Security Act Manual (5th Edition). U.S. Department of Agriculture, NRCS .
Vaiphasa, C. 2006. Consideration of smoothing techniques for hyperspectral remote sensing. ISPRS Journal of Photogrammetry and Remote Sensing 60: 91–99.
Venteris, E.R., G.W. McCarty, J.C. Ritchie, and T. Gish. 2004. Influence of Management History and Landscape Variables on Soil Organic Carbon and Soil Redistribution. Soil Science 169(11): 787–795.
Weltzin, J.F., C. Harth, S.D. Bridgham, J. Pastor, and M. Vonderharr. 2001. Production and microtopography of bog bryophytes: response to warming and water-table manipulations. Oecologia 128: 557-565.
Wiesmeier, M., P. Spörlein, U. Geub, E. Hangen, S. Haug, A. Reischl, B. Schilling, M. von Lützow, and I. Kögel-Knabner. 2012. Soil organic carbon stocks in southeast Germany (Bavaria) as affected by land use, soil type and sampling depth. Global Change Biology 18: 2233–2245.
Wu, A.M. 2014. Hillslope Redistribution of Soil Organic Carbon in the Depressional Landscape in Minnesota. Doctor of Philosophy, Minneapolis, Minnesota: University of Minnesota.
Zedler, J.B. 2003. Wetlands at Your Service: Reducing Impacts of Agriculture at the Watershed Scale. *Front. Ecol. Environ.* 1: 65–72.

Appendix A – Statistics on Pedotransfer Function Training Data

Table 1. *Bulk density average and standard deviation of training data*

Training Data	**Bulk Density**					
	Average			**Standard Deviation**		
	Texture			Texture		
Horizon	S	L	C	S	L	C
Ap	---	1.561628	---	---	0.17992	---
A or AB (directly under Ap)	---	1.574	---	---	0.110589	---
CB + C	1.688571	1.814	---	0.109762	0.055498	---
BC	1.719167	1.6625	---	0.096621	0.176328	---
B	1.690769	1.643696	1.76	0.142036	0.221032	0
Bt + BCt	1.614286	1.676207	1.765	0.152737	0.134468	0.035355
E	1.68	1.653333	---	0.098995	0.280416	---

Table 2. *Soil Organic Carbon average and standard deviation of data*

Training Data	**Soil Organic Carbon**					
	Average			**Standard Deviation**		
	Texture			Texture		
Horizon	S	L	C	S	L	C
Ap	---	1.167368	---	---	1.040088	---
A or AB (directly under Ap)	---	0.532	---	---	0.453949	---
CB + C	0.042857	0.21	---	0.031472	0.19799	---
BC	0.09	0.18	---	0.085706	0.127279	---
B	0.092308	0.354565	0.06	0.110314	0.564674	0
Bt + BCt	0.151429	0.240455	0.09	0.049809	0.196747	0.042426
E	0.185	0.445	---	0.049497	0.091924	---

This Study's Data	**Soil Organic Carbon**					
	Average			**Standard Deviation**		
	Texture			Texture		
Horizon	S	L	C	S	L	C
Ap	0.954421	1.269699	---	0	0.556906	---
A	0.588549	1.040234	---	0	0.469024	---
B	0.101	0.348286	---	0.078412	0.606866	---
Bt	---	0.497072	---	---	0.602241	---

Table 3. *Bulk density statistics of training data after B and BC horizons were combined.*

Training Data	**Bulk Density**					
	Average			**Standard Deviation**		
	Texture			Texture		
Horizon	S	L	C	S	L	C
Ap	---	1.561628	---	---	0.17992	---
A or AB (directly under Ap)	---	1.574	---	---	0.110589	---
CB + C	1.688571	1.814	---	0.109762	0.055498	---
B + BC	1.7044	1.6452	1.76	0.12073	0.216326	0
Bt + BCt	1.614286	1.676207	1.765	0.152737	0.134468	0.035355
E	1.68	1.653333	---	0.098995	0.280416	---

Appendix B – Correlation Between Terrain Attributes and SOC

Table 1. *Correlation of continuous terrain variables to Bay SOC stock*

Continuous Variables	Pearson's Correlation Coefficient (r)
1. Ditch Width Average (m)	0.647
2. Ditch Depth Average (m)	0.736
3. Elevation (m)	0.476
4. Bay Area (ha)	0.300
5. Upslope Catchment Area (m)	0.088
6. Upslope Catchment Area to Bay Area ratio	-0.161
7. Average NDVI	-0.409
8. Minimum NDVI	-0.320
9. Maximum NDVI	0.117
10. Average Aquifer Thickness (m)	-0.061
11. Minimum Aquifer Thickness (m)	-0.055
12. Maximum Aquifer Thickness (m)	-0.064
13. Bay Slope Average (percent rise)	-0.032
14. Bay Slope Maximum (percent rise)	0.137
15. Upslope Catchment Area Total Curvature Average	0.153
16. Upslope Catchment Area Total Curvature Minimum	-0.022
17. Upslope Catchment Area Total Curvature Maximum	0.292
18. Upslope Catchment Area Planar Curvature Average	0.152
19. Upslope Catchment Area Planar Curvature Minimum	-0.036
20. Upslope Catchment Area Planar Curvature Maximum	0.267
21. Upslope Catchment Area Profile Curvature Average	0.064
22. Upslope Catchment Area Profile Curvature Minimum	-0.169
23. Upslope Catchment Area Profile Curvature Maximum	0.182
24. Upslope Catchment Area Tangential Curvature Average	0.144
25. Upslope Catchment Area Tangential Curvature Minimum	-0.053
26. Upslope Catchment Area Tangential Curvature Maximum	0.197
27. Bay Total Curvature Average	0.088
28. Bay Total Curvature Minimum	-0.318
29. Bay Total Curvature Maximum	0.488
30. Bay Planar Curvature Average	-0.139
31. Bay Planar Curvature Minimum	-0.160
32. Bay Planar Curvature Maximum	0.428
33. Bay Profile Curvature Average	-0.229
34. Bay Profile Curvature Minimum	-0.447
35. Bay Profile Curvature Maximum	0.252
36. Bay Tangential Curvature Average	-0.197
37. Bay Tangential Curvature Minimum	-0.544
38. Bay Tangential Curvature Maximum	0.496
39. Upslope Catchment Area Maximum Flow Path Length (m)	-0.072
40. TWI Average	-0.088
41. TCI Average	-0.092

Table 2. *Correlation of non-continuous terrain variables to Bay SOC stock*

Binary and Categorical Data	Spearman's Rank Correlation Coefficient	p-value
42. Grey Redox Depletions	0.069	0.7
43. Redox Iron Concentrations	0.226	0.2
44. Freestanding Water within the First Meter	0.158	0.4
45. Known Drainage	0.495	0.007
46. Pipes	0.102	0.6
47. Tile Drain	0.131	0.5
48. Ditches	0.474	0.01
49. Bay Overlap	0.233	0.2
50. Sampled Soil Series	-0.154	0.4

Appendix C – Pearson's Correlation Coefficient of Continuous Terrain Attributes

All terrain attribute pairs with a Pearson's correlation coefficient greater than 0.5 are in bold italics. A terrain attribute abbreviation key is on page 60.

	DWA	DDA	Elevation	BA	UA	UA:BA	NDVI_avg	NDVI_min	NDVI_max
DWA	1	***0.695***	0.343	***0.641***	0.275	-0.098	-0.223	-0.246	0.086
DDA	***0.695***	1	0.161	0.140	-0.020	-0.088	-0.379	-0.293	0.057
Elevation	0.343	0.161	1	0.317	0.163	-0.358	-0.026	0.088	0.225
BA	***0.641***	0.140	0.317	1	***0.518***	-0.156	0.035	-0.200	0.224
UA	0.275	-0.020	0.163	***0.518***	1	0.498	-0.052	0.026	-0.147
UA:BA	-0.098	-0.088	-0.358	-0.156	0.498	1	-0.230	0.065	***-0.623***
NDVI_avg	-0.223	-0.379	-0.026	0.035	-0.052	-0.230	1	0.357	0.244
NDVI_min	-0.246	-0.293	0.088	-0.200	0.026	0.065	0.357	1	-0.321
NDVI_max	0.086	0.057	0.225	0.224	-0.147	***-0.623***	0.244	-0.321	1
AQ_thck_avg	0.186	0.137	0.282	0.302	0.323	0.054	0.236	0.230	-0.109
AQ_thck_min	0.203	0.137	0.297	0.317	0.327	0.051	0.228	0.229	-0.108
AQ_thck_max	0.179	0.132	0.264	0.316	0.326	0.042	0.253	0.219	-0.099
BaySlope_avg	-0.105	0.108	-0.163	-0.048	-0.175	-0.346	-0.036	0.040	-0.130
BaySlope_max	0.083	-0.024	0.109	0.273	0.429	0.149	-0.209	-0.188	-0.249
UATotalC_avg	-0.077	-0.050	-0.289	-0.110	-0.155	-0.086	0.209	-0.175	0.268
UATotalC_min	-0.222	-0.040	-0.106	-0.411	-0.524	-0.284	-0.008	0.066	-0.030
UATotalC_max	0.297	0.192	0.249	0.262	***0.568***	0.367	-0.291	-0.174	0.017
UAPlanarC_avg	0.296	0.098	***0.508***	0.104	-0.038	-0.142	0.085	0.096	0.266
UAPlanarC_min	-0.274	-0.143	0.103	-0.257	-0.565	-0.547	0.218	0.251	0.094
UAPlanarC_max	0.257	0.078	0.292	0.267	***0.556***	0.274	-0.245	-0.170	0.134
UAProfileC_avg	0.198	-0.072	0.419	0.102	0.132	0.119	-0.007	0.034	0.182
UAProfileC_min	-0.187	-0.154	-0.176	-0.237	-0.621	-0.355	0.188	0.149	0.006
UAProfileC_max	0.259	0.099	0.268	0.375	***0.529***	0.293	-0.083	-0.118	0.057
UATanC_avg	0.300	0.238	0.369	0.111	0.053	-0.078	-0.079	-0.124	0.240
UATanC_min	-0.209	-0.070	0.031	-0.344	***-0.532***	-0.358	0.214	0.178	0.227
UATanC_max	0.252	0.069	0.193	0.308	***0.573***	0.303	-0.270	-0.184	-0.138
BayTotalC_avg	0.227	-0.008	0.393	0.395	0.199	-0.217	0.161	-0.007	0.422
BayTotalC_min	-0.326	-0.262	-0.212	-0.358	-0.341	0.099	-0.057	0.285	-0.237
BayTotalC_max	0.460	0.475	0.459	0.148	0.215	-0.104	-0.384	-0.104	0.110
BayPlanarC_avg	-0.049	-0.082	0.104	-0.097	-0.101	-0.084	0.094	0.146	0.143
BayPlanarC_min	-0.254	-0.189	-0.188	-0.316	-0.371	0.069	0.091	0.234	-0.159
BayPlanarC_max	0.428	0.456	0.346	0.188	0.197	-0.136	-0.259	-0.170	0.182
BayProfileC_avg	-0.176	-0.104	-0.061	-0.319	-0.208	0.014	0.053	0.203	-0.039
BayProfileC_min	-0.463	-0.372	-0.473	-0.286	-0.245	0.150	0.348	0.141	-0.172
BayProfileC_max	0.337	0.254	0.254	0.227	0.250	-0.111	-0.062	-0.204	0.201
BayTanC_avg	-0.115	-0.229	0.094	-0.066	-0.070	-0.079	0.142	0.125	0.184
BayTanC_min	-0.478	***-0.794***	0.009	-0.155	-0.111	0.096	0.262	0.344	-0.038
BayTanC_max	***0.508***	0.418	0.274	0.341	0.345	-0.146	-0.368	-0.295	0.028
UAFlowPath	0.252	-0.065	-0.007	0.218	***0.810***	***0.723***	-0.140	0.076	-0.354
TWI_avg	-0.174	-0.332	0.008	0.085	0.176	0.129	0.111	0.095	-0.090
TCI	-0.218	-0.380	-0.048	0.134	0.152	0.093	0.123	0.112	0.034

	AQ_thck_avg	AQ_thck_min	AQ_thck_max	BaySlope_avg	BaySlope_max	UATotalC_avg
DWA	0.186	0.203	0.179	-0.105	0.083	-0.077
DDA	0.137	0.137	0.132	0.108	-0.024	-0.050
Elevation	0.282	0.297	0.264	-0.163	0.109	-0.289
BA	0.302	0.317	0.316	-0.048	0.273	-0.110
UA	0.323	0.327	0.326	-0.175	0.429	-0.155
UA:BA	0.054	0.051	0.042	-0.346	0.149	-0.086
NDVI_avg	0.236	0.228	0.253	-0.036	-0.209	0.209
NDVI_min	0.230	0.229	0.219	0.040	-0.188	-0.175
NDVI_max	-0.109	-0.108	-0.099	-0.130	-0.249	0.268
AQ_thck_avg	1	***0.995***	***0.996***	-0.060	0.220	-0.347
AQ_thck_min	***0.995***	1	***0.988***	-0.107	0.206	-0.346
AQ_thck_max	***0.996***	***0.988***	1	-0.026	0.223	-0.343
BaySlope_avg	-0.060	-0.107	-0.026	1	0.297	-0.173
BaySlope_max	0.220	0.206	0.223	0.297	1	-0.130
UATotalC_avg	-0.347	-0.346	-0.343	-0.173	-0.130	1
UATotalC_min	-0.378	-0.388	-0.371	0.433	-0.319	0.130
UATotalC_max	0.224	0.252	0.199	-0.492	0.410	-0.143
UAPlanarC_avg	0.296	0.335	0.270	***-0.732***	-0.355	-0.037
UAPlanarC_min	-0.239	-0.259	-0.234	0.447	-0.249	0.165
UAPlanarC_max	0.023	0.052	0.005	***-0.563***	0.333	-0.073
UAProfileC_avg	0.182	0.225	0.142	***-0.887***	-0.210	-0.097
UAProfileC_min	-0.300	-0.311	-0.284	0.272	***-0.608***	0.144
UAProfileC_max	0.308	0.318	0.302	***-0.509***	0.318	-0.098
UATanC_avg	0.330	0.367	0.312	***-0.605***	-0.139	-0.122
UATanC_min	-0.299	-0.288	-0.291	-0.022	***-0.768***	0.230
UATanC_max	0.237	0.249	0.219	-0.132	***0.804***	-0.165
BayTotalC_avg	0.122	0.168	0.101	***-0.545***	-0.010	-0.095
BayTotalC_min	-0.201	-0.204	-0.195	0.261	-0.322	-0.138
BayTotalC_max	0.005	0.055	-0.025	-0.319	0.120	-0.215
BayPlanarC_avg	-0.281	-0.246	-0.304	-0.307	-0.209	-0.132
BayPlanarC_min	-0.280	-0.303	-0.267	0.253	-0.345	0.061
BayPlanarC_max	0.016	0.066	-0.003	-0.348	0.002	-0.137
BayProfileC_avg	-0.386	-0.366	-0.403	-0.118	-0.265	-0.125
BayProfileC_min	0.011	-0.033	0.032	0.261	-0.331	0.127
BayProfileC_max	0.183	0.209	0.167	-0.358	0.201	0.072
BayTanC_avg	-0.245	-0.204	-0.269	-0.413	-0.182	-0.069
BayTanC_min	-0.266	-0.255	-0.272	-0.197	-0.256	-0.046
BayTanC_max	0.062	0.089	0.055	-0.028	0.404	-0.107
UAFlowPath	0.214	0.226	0.190	-0.384	0.296	-0.178
TWI_avg	0.275	0.264	0.280	-0.001	0.243	0.186
TCI	0.149	0.122	0.158	0.055	0.142	0.229

	UATotalC_min	UATotalC_max	UAPlanarC_avg	UAPlanarC_min	UAPlanarC_max
DWA	-0.222	0.297	0.296	-0.274	0.257
DDA	-0.040	0.192	0.098	-0.143	0.078
Elevation	-0.106	0.249	***0.508***	0.103	0.292
BA	-0.411	0.262	0.104	-0.257	0.267
UA	***-0.524***	***0.568***	-0.038	***-0.565***	***0.556***
UA:BA	-0.284	0.367	-0.142	***-0.547***	0.274
NDVI_avg	-0.008	-0.291	0.085	0.218	-0.245
NDVI_min	0.066	-0.174	0.096	0.251	-0.170
NDVI_max	-0.030	0.017	0.266	0.094	0.134
AQ_thck_avg	-0.378	0.224	0.296	-0.239	0.023
AQ_thck_min	-0.388	0.252	0.335	-0.259	0.052
AQ_thck_max	-0.371	0.199	0.270	-0.234	0.005
BaySlope_avg	0.433	-0.492	***-0.732***	0.447	***-0.563***
BaySlope_max	-0.319	0.410	-0.355	-0.249	0.333
UATotalC_avg	0.130	-0.143	-0.037	0.165	-0.073
UATotalC_min	1	***-0.696***	-0.320	***0.809***	***-0.709***
UATotalC_max	***-0.696***	1	0.331	***-0.762***	***0.919***
UAPlanarC_avg	-0.320	0.331	1	-0.167	0.405
UAPlanarC_min	***0.809***	***-0.762***	-0.167	1	***-0.692***
UAPlanarC_max	***-0.709***	***0.919***	0.405	***-0.692***	1
UAProfileC_avg	-0.462	***0.532***	***0.868***	-0.398	***0.601***
UAProfileC_min	***0.714***	***-0.915***	-0.110	**0.703**	***-0.816***
UAProfileC_max	***-0.815***	***0.855***	0.445	***-0.681***	***0.832***
UATanC_avg	***-0.535***	***0.533***	***0.859***	-0.396	***0.571***
UATanC_min	***0.708***	***-0.573***	0.222	***0.686***	***-0.506***
UATanC_max	***-0.582***	***0.827***	-0.005	***-0.600***	***0.713***
BayTotalC_avg	-0.384	0.398	***0.557***	-0.126	***0.521***
BayTotalC_min	***0.697***	***-0.631***	-0.275	0.471	***-0.660***
BayTotalC_max	-0.327	***0.601***	0.418	-0.302	***0.650***
BayPlanarC_avg	0.011	0.115	0.243	0.125	0.235
BayPlanarC_min	***0.708***	***-0.678***	-0.288	***0.530***	***-0.708***
BayPlanarC_max	-0.370	***0.538***	0.438	-0.306	***0.606***
BayProfileC_avg	0.196	-0.056	0.036	0.211	0.033
BayProfileC_min	0.405	***-0.590***	-0.342	0.289	***-0.666***
BayProfileC_max	***-0.553***	***0.662***	0.460	-0.417	***0.692***
BayTanC_avg	-0.030	0.124	0.309	0.122	0.255
BayTanC_min	0.305	-0.347	0.058	0.324	-0.201
BayTanC_max	-0.314	0.467	0.150	-0.240	***0.503***
UAFlowPath	-0.476	***0.617***	0.105	***-0.658***	***0.565***
TWI_avg	-0.048	-0.024	-0.016	-0.016	-0.099
TCI	-0.013	-0.167	-0.134	0.061	-0.194

	UAProfileC_avg	UAProfileC_min	UAProfileC_max	UATanC_avg	UATanC_min
DWA	0.198	-0.187	0.259	0.300	-0.209
DDA	-0.072	-0.154	0.099	0.238	-0.070
Elevation	0.419	-0.176	0.268	0.369	0.031
BA	0.102	-0.237	0.375	0.111	-0.344
UA	0.132	***-0.621***	***0.529***	0.053	***-0.532***
UA:BA	0.119	-0.355	0.293	-0.078	-0.358
NDVI_avg	-0.007	0.188	-0.083	-0.079	0.214
NDVI_min	0.034	0.149	-0.118	-0.124	0.178
NDVI_max	0.182	0.006	0.057	0.240	0.227
AQ_thck_avg	0.182	-0.300	0.308	0.330	-0.299
AQ_thck_min	0.225	-0.311	0.318	0.367	-0.288
AQ_thck_max	0.142	-0.284	0.302	0.312	-0.291
BaySlope_avg	***-0.887***	0.272	***-0.509***	***-0.605***	-0.022
BaySlope_max	-0.210	***-0.608***	0.318	-0.139	***-0.768***
UATotalC_avg	-0.097	0.144	-0.098	-0.122	0.230
UATotalC_min	-0.462	***0.714***	***-0.815***	***-0.535***	***0.708***
UATotalC_max	***0.532***	***-0.915***	***0.855***	***0.533***	***-0.573***
UAPlanarC_avg	***0.868***	-0.110	0.445	***0.859***	0.222
UAPlanarC_min	-0.398	***0.703***	***-0.681***	-0.396	***0.686***
UAPlanarC_max	***0.601***	***-0.816***	***0.832***	***0.571***	***-0.506***
UAProfileC_avg	1	-0.324	***0.570***	***0.751***	0.002
UAProfileC_min	-0.324	1	***-0.822***	-0.386	***0.702***
UAProfileC_max	***0.570***	***-0.822***	1	***0.626***	-0.490
UATanC_avg	***0.751***	-0.386	***0.626***	1	-0.020
UATanC_min	0.002	***0.702***	-0.490	-0.020	1
UATanC_max	0.222	***-0.905***	***0.684***	0.213	***-0.790***
BayTotalC_avg	***0.651***	-0.369	0.464	***0.520***	-0.045
BayTotalC_min	-0.297	***0.671***	***-0.711***	-0.492	0.495
BayTotalC_max	0.468	***-0.511***	0.423	***0.569***	-0.183
BayPlanarC_avg	0.343	-0.126	0.120	0.248	0.199
BayPlanarC_min	-0.344	***0.715***	***-0.664***	***-0.598***	***0.508***
BayPlanarC_max	0.432	-0.446	0.418	***0.625***	-0.121
BayProfileC_avg	0.112	0.028	-0.077	0.057	0.270
BayProfileC_min	-0.427	***0.590***	-0.499	***-0.508***	0.310
BayProfileC_max	0.445	***-0.648***	***0.669***	***0.676***	-0.319
BayTanC_avg	0.436	-0.120	0.127	0.282	0.204
BayTanC_min	0.151	0.428	-0.324	-0.221	0.361
BayTanC_max	0.154	-0.464	0.331	0.373	-0.349
UAFlowPath	0.349	***-0.597***	***0.521***	0.148	-0.498
TWI_avg	0.007	0.036	0.020	-0.150	-0.074
TCI	-0.096	0.175	-0.107	-0.295	-0.042

	UATanC_max	BayTotalC_avg	BayTotalC_min	BayTotalC_max	BayPlanarC_avg
DWA	0.252	0.227	-0.326	0.460	-0.049
DDA	0.069	-0.008	-0.262	0.475	-0.082
Elevation	0.193	0.393	-0.212	0.459	0.104
BA	0.308	0.395	-0.358	0.148	-0.097
UA	***0.573***	0.199	-0.341	0.215	-0.101
UA:BA	0.303	-0.217	0.099	-0.104	-0.084
NDVI_avg	-0.270	0.161	-0.057	-0.384	0.094
NDVI_min	-0.184	-0.007	0.285	-0.104	0.146
NDVI_max	-0.138	0.422	-0.237	0.110	0.143
AQ_thck_avg	0.237	0.122	-0.201	0.005	-0.281
AQ_thck_min	0.249	0.168	-0.204	0.055	-0.246
AQ_thck_max	0.219	0.101	-0.195	-0.025	-0.304
BaySlope_avg	-0.132	***-0.545***	0.261	-0.319	-0.307
BaySlope_max	***0.804***	-0.010	-0.322	0.120	-0.209
UATotalC_avg	-0.165	-0.095	-0.138	-0.215	-0.132
UATotalC_min	***-0.582***	-0.384	***0.697***	-0.327	0.011
UATotalC_max	***0.827***	0.398	***-0.631***	***0.601***	0.115
UAPlanarC_avg	-0.005	***0.557***	-0.275	0.418	0.243
UAPlanarC_min	***-0.600***	-0.126	0.471	-0.302	0.125
UAPlanarC_max	***0.713***	***0.521***	***-0.660***	***0.650***	0.235
UAProfileC_avg	0.222	***0.651***	-0.297	0.468	0.343
UAProfileC_min	***-0.905***	-0.369	***0.671***	***-0.511***	-0.126
UAProfileC_max	***0.684***	0.464	***-0.711***	0.423	0.120
UATanC_avg	0.213	***0.520***	-0.492	***0.569***	0.248
UATanC_min	***-0.790***	-0.045	0.495	-0.183	0.199
UATanC_max	1	0.261	***-0.559***	0.427	0.034
BayTotalC_avg	0.261	1	-0.472	***0.552***	***0.621***
BayTotalC_min	***-0.559***	-0.472	1	***-0.531***	-0.187
BayTotalC_max	0.427	***0.552***	***-0.531***	1	***0.506***
BayPlanarC_avg	0.034	***0.621***	-0.187	***0.506***	1
BayPlanarC_min	***-0.574***	***-0.502***	***0.855***	***-0.645***	-0.209
BayPlanarC_max	0.313	***0.577***	***-0.627***	***0.944***	***0.559***
BayProfileC_avg	-0.096	0.267	0.001	0.348	***0.921***
BayProfileC_min	***-0.550***	***-0.614***	***0.552***	***-0.913***	-0.486
BayProfileC_max	***0.536***	***0.535***	***-0.869***	***0.691***	0.380
BayTanC_avg	0.050	***0.685***	-0.175	0.460	***0.953***
BayTanC_min	-0.341	0.020	***0.602***	-0.434	0.145
BayTanC_max	***0.509***	0.373	***-0.620***	***0.789***	0.267
UAFlowPath	***0.595***	0.128	-0.191	0.181	-0.031
TWI_avg	0.073	-0.253	0.266	-0.491	***-0.743***
TCI	-0.074	-0.303	0.346	***-0.598***	***-0.696***

	BayPlanarC_min	BayPlanarC_max	BayProfileC_avg	BayProfileC_min	BayProfileC_max
DWA	-0.254	0.428	-0.176	-0.463	0.337
DDA	-0.189	0.456	-0.104	-0.372	0.254
Elevation	-0.188	0.346	-0.061	-0.473	0.254
BA	-0.316	0.188	-0.319	-0.286	0.227
UA	-0.371	0.197	-0.208	-0.245	0.250
UA:BA	0.069	-0.136	0.014	0.150	-0.111
NDVI_avg	0.091	-0.259	0.053	0.348	-0.062
NDVI_min	0.234	-0.170	0.203	0.141	-0.204
NDVI_max	-0.159	0.182	-0.039	-0.172	0.201
AQ_thck_avg	-0.280	0.016	-0.386	0.011	0.183
AQ_thck_min	-0.303	0.066	-0.366	-0.033	0.209
AQ_thck_max	-0.267	-0.003	-0.403	0.032	0.167
BaySlope_avg	0.253	-0.348	-0.118	0.261	-0.358
BaySlope_max	-0.345	0.002	-0.265	-0.331	0.201
UATotalC_avg	0.061	-0.137	-0.125	0.127	0.072
UATotalC_min	***0.708***	-0.370	0.196	0.405	***-0.553***
UATotalC_max	***-0.678***	***0.538***	-0.056	***-0.590***	***0.662***
UAPlanarC_avg	-0.288	0.438	0.036	-0.342	0.460
UAPlanarC_min	***0.530***	-0.306	0.211	0.289	-0.417
UAPlanarC_max	***-0.708***	***0.606***	0.033	***-0.666***	***0.692***
UAProfileC_avg	-0.344	0.432	0.112	-0.427	0.445
UAProfileC_min	***0.715***	-0.446	0.028	***0.590***	***-0.648***
UAProfileC_max	***-0.664***	0.418	-0.077	-0.499	***0.669***
UATanC_avg	***-0.598***	***0.625***	0.057	***-0.508***	***0.676***
UATanC_min	***0.508***	-0.121	0.270	0.310	-0.319
UATanC_max	***-0.574***	0.313	-0.096	***-0.550***	***0.536***
BayTotalC_avg	***-0.502***	***0.577***	0.267	***-0.614***	***0.535***
BayTotalC_min	***0.855***	***-0.627***	0.001	***0.552***	***-0.869***
BayTotalC_max	***-0.645***	***0.944***	0.348	***-0.913***	***0.691***
BayPlanarC_avg	-0.209	***0.559***	***0.921***	-0.486	0.380
BayPlanarC_min	1	***-0.700***	-0.014	***0.653***	***-0.869***
BayPlanarC_max	***-0.700***	1	0.402	***-0.820***	***0.760***
BayProfileC_avg	-0.014	0.402	1	-0.288	0.205
BayProfileC_min	***0.653***	***-0.820***	-0.288	1	***-0.676***
BayProfileC_max	***-0.869***	***0.760***	0.205	***-0.676***	1
BayTanC_avg	-0.221	***0.524***	***0.831***	-0.453	0.340
BayTanC_min	***0.510***	-0.457	0.174	0.387	***-0.507***
BayTanC_max	***-0.675***	***0.810***	0.138	***-0.744***	***0.648***
UAFlowPath	-0.262	0.098	-0.086	-0.161	0.222
TWI_avg	0.250	***-0.598***	***-0.786***	0.389	-0.401
TCI	0.375	***-0.659***	***-0.705***	0.491	***-0.557***

	BayTanC_avg	BayTanC_min	BayTanC_max	UAFlowPath	TWI_mean	TCI
DWA	-0.115	-0.478	***0.508***	0.252	-0.174	-0.218
DDA	-0.229	***-0.794***	0.418	-0.065	-0.332	-0.380
Elevation	0.094	0.009	0.274	-0.007	0.008	-0.048
BA	-0.066	-0.155	0.341	0.218	0.085	0.134
UA	-0.070	-0.111	0.345	***0.810***	0.176	0.152
UA:BA	-0.079	0.096	-0.146	***0.723***	0.129	0.093
NDVI_avg	0.142	0.262	-0.368	-0.140	0.111	0.123
NDVI_min	0.125	0.344	-0.295	0.076	0.095	0.112
NDVI_max	0.184	-0.038	0.028	-0.354	-0.090	0.034
AQ_thck_avg	-0.245	-0.266	0.062	0.214	0.275	0.149
AQ_thck_min	-0.204	-0.255	0.089	0.226	0.264	0.122
AQ_thck_max	-0.269	-0.272	0.055	0.190	0.280	0.158
BaySlope_avg	-0.413	-0.197	-0.028	-0.384	-0.001	0.055
BaySlope_max	-0.182	-0.256	0.404	0.296	0.243	0.142
UATotalC_avg	-0.069	-0.046	-0.107	-0.178	0.186	0.229
UATotalC_min	-0.030	0.305	-0.314	-0.476	-0.048	-0.013
UATotalC_max	0.124	-0.347	0.467	***0.617***	-0.024	-0.167
UAPlanarC_avg	0.309	0.058	0.150	0.105	-0.016	-0.134
UAPlanarC_min	0.122	0.324	-0.240	***-0.658***	-0.016	0.061
UAPlanarC_max	0.255	-0.201	***0.503***	***0.565***	-0.099	-0.194
UAProfileC_avg	0.436	0.151	0.154	0.349	0.007	-0.096
UAProfileC_min	-0.120	0.428	-0.464	***-0.597***	0.036	0.175
UAProfileC_max	0.127	-0.324	0.331	***0.521***	0.020	-0.107
UATanC_avg	0.282	-0.221	0.373	0.148	-0.150	-0.295
UATanC_min	0.204	0.361	-0.349	-0.498	-0.074	-0.042
UATanC_max	0.050	-0.341	**0.509**	***0.595***	0.073	-0.074
BayTotalC_avg	***0.685***	0.020	0.373	0.128	-0.253	-0.303
BayTotalC_min	-0.175	***0.602***	***-0.620***	-0.191	0.266	0.346
BayTotalC_max	0.460	-0.434	***0.789***	0.181	-0.491	***-0.598***
BayPlanarC_avg	***0.953***	0.145	0.267	-0.031	***-0.743***	***-0.696***
BayPlanarC_min	-0.221	***0.510***	***-0.675***	-0.262	0.250	0.375
BayPlanarC_max	***0.524***	-0.457	***0.810***	0.098	***-0.598***	***-0.659***
BayProfileC_avg	***0.831***	0.174	0.138	-0.086	***-0.786***	***-0.705***
BayProfileC_min	-0.453	0.387	***-0.744***	-0.161	0.389	0.491
BayProfileC_max	0.340	***-0.507***	***0.648***	0.222	-0.401	***-0.557***
BayTanC_avg	1	0.261	0.292	-0.004	***-0.568***	***-0.514***
BayTanC_min	0.261	1	***-0.546***	0.006	0.254	0.353
BayTanC_max	0.292	***-0.546***	1	0.185	-0.340	-0.392
UAFlowPath	-0.004	0.006	0.185	1	0.175	0.071
TWI_avg	***-0.568***	0.254	-0.340	0.175	1	***0.905***
TCI	***-0.514***	0.353	-0.392	0.071	***0.905***	1

Continuous Terrain Attribute Abbreviation Key

DWA – Ditch Width Average
DDA – Ditch Depth Average
BA – Bay Area
UA – Upslope Catchment Area
AQ_thick – Aquifer Thickness
UATotalC – Upslope Catchment Area Total Curvature
UAPlanarC – Upslope Catchment Area Planar Curvature
UAProfileC – Upslope Catchment Area Profile Curvature
UATanC – Upslope Catchment Area Tangential Curvature
BayTotalC – Bay Total Curvature
BayPlanarC – Bay Planar Curvature
BayProfileC – Bay Profile Curvature
BayTanC – Bay Tangential Curvature
UAFlowPath – Upslope Catchment Area Maximum Flow Path Length

Appendix D – Correlations of Categorical Terrain Attributes

Table 1. *Significant correlations of terrain attributes with ditches (p-value ≤0.05)*

Terrain Attributes	Spearman's Rank Correlation Coefficient	p-value
Freestanding Water Encountered within the First Meter	0.479	0.01
Known Drainage	0.706	0.00003
Ditch Width	0.99	0.0000
Ditch Depth	0.996	0.0000
Elevation	0.377	0.05
Bay Area	0.529	0.004
Upslope Catchment Area Total Curvature Maximum	0.406	0.03
Upslope Catchment Area Profile Curvature Minimum	-0.382	0.04
Bay Total Curvature Maximum	0.426	0.02
Bay Planar Curvature Maximum	0.474	0.01
Bay Profile Curvature Minimum	-0.523	0.004
Bay Profile Curvature Maximum	0.446	0.02
Bay Tangential Curvature Maximum	0.486	0.009

Table 2. *Significant correlations of terrain attributes with known drainage (p-value ≤0.05)*

Terrain Attributes	Spearman's Rank Correlation Coefficient	p-value
Freestanding Water Encountered within the First Meter	0.429	0.02
Pipes	0.48	0.01
Ditches	0.706	0.00003
Ditch Width Average	0.705	0.00003
Ditch Depth Average	0.704	0.00003
Elevation	0.455	0.02
Bay Area	0.567	0.002
Upslope Catchment Area	0.444	0.02
Upslope Catchment Area Total Curvature Minimum	-0.434	0.02
Upslope Catchment Area Planar Curvature Minimum	-0.383	0.04
Upslope Catchment Area Planar Curvature Maximum	0.434	0.02
Upslope Catchment Area Profile Curvature Maximum	-0.454	0.02
Bay Total Curvature Minimum	-0.424	0.02
Bay Tangential Curvature Maximum	0.424	0.02

Table 3. *Significant correlations of terrain attributes with pipes (p-value ≤0.05)*

Terrain Attributes	Spearman's Rank Correlation Coefficient	p-value
Known Drainage	0.48	0.01
NDVI Maximum	0.437	0.02

Table 4. *Significant correlations of terrain attributes with water hit (p-value ≤0.05)*

Terrain Attributes	Spearman's Rank Correlation Coefficient	p-value
Known Drainage	0.429	0.02
Ditches	0.479	0.01
Ditch Width Average	0.47	0.01
Ditch Depth Average	0.478	0.01
Bay Area	0.424	0.02
NDVI Minimum	-0.434	0.02
NDVI Maximum	0.419	0.03
Bay Total Curvature Average	0.434	0.02
Bay Planar Curvature Maximum	0.373	0.05

Table 5. *Significant correlations of terrain attributes with grey redox depletions (p-value ≤0.05)*

Terrain Attributes	Spearman's Rank Correlation Coefficient	p-value
Bay Slope Average	-0.447	0.02
Upslope Catchment Area Total Curvature Average	-0.378	0.05
Upslope Catchment Area Total Curvature Minimum	-0.446	0.02
Upslope Catchment Area Total Curvature Maximum	0.446	0.02
Upslope Catchment Area Planar Curvature Average	0.446	0.02
Upslope Catchment Area Planar Curvature Minimum	-0.446	0.02
Upslope Catchment Area Planar Curvature Maximum	0.446	0.02
Upslope Catchment Area Profile Curvature Average	0.446	0.02
Upslope Catchment Area Profile Curvature Minimum	-0.446	0.02
Upslope Catchment Area Profile Curvature Maximum	0.446	0.02
Upslope Catchment Area Tangential Curvature Average	0.446	0.02
Upslope Catchment Area Tangential Curvature Maximum	0.429	0.02
Bay Total Curvature Average	0.395	0.04
Bay Total Curvature Minimum	-0.447	0.02
Bay Total Curvature Maximum	0.446	0.02
Bay Planar Curvature Average	0.446	0.02
Bay Planar Curvature Minimum	-0.447	0.02
Bay Planar Curvature Maximum	0.446	0.02
Bay Profile Curvature Minimum	-0.446	0.02
Bay Profile Curvature Maximum	0.446	0.02
Bay Tangential Curvature Average	0.395	0.04
Bay Tangential Curvature Minimum	-0.429	0.02
Bay Tangential Curvature Maximum	0.446	0.02
TWI Average	-0.369	0.05
TCI	-0.429	0.02

Table 6. *Significant correlations of terrain attributes with bay overlap (p-value ≤0.05)*

Terrain Attributes	Spearman's Rank Correlation Coefficient	p-value
Bay Area	0.487	0.009
Upslope Area	0.5	0.007
Aquifer Thickness Average	0.471	0.01
Aquifer Thickness Minimum	0.417	0.03
Aquifer Thickness Maximum	0.503	0.006
Bay Slope Maximum	0.48	0.01
Upslope Catchment Area Total Curvature Minimum	-0.372	0.05
Upslope Catchment Area Total Curvature Maximum	0.376	0.05
Upslope Catchment Area Planar Curvature Minimum	-0.422	0.03
Upslope Catchment Area Planar Curvature Maximum	0.43	0.02
Upslope Catchment Area Profile Curvature Minimum	-0.37	0.05
Bay Profile Curvature Average	-0.367	0.05
Upslope Catchment Area Maximum Flow Path Length	0.385	0.04

Appendix E – Soil Profile Descriptions with Pictures

All markers in pictures indicate augered depth in 20 cm increments. Textural class is reported as field texture.

P6B20S1

Caroline County

Mapped Soil Series: Lenni

Horizon	Depth (cm)	Texture	Matrix Color
Ap1	27	Loam	10YR 5/3
Ap2	44	Clay Loam	10YR 5/3
Bg	68	Sandy Clay Loam	10YR 7/1
Bgt1	86	Silty Clay Loam	10YR 7/1
Btg2	100+	Silty Clay Loam	7.5YR 6/1

Additional Notes

Depth to grey redox depletions: 44 cm

Depth to redox iron concentrations: 44 cm

P6B20S2

Caroline County

Mapped Soil Series: Lenni

Horizon	Depth (cm)	Texture	Matrix Color
Ap	20	Loam	10YR 5/3
A	46	Sandy Loam	10YR 5/3
B	67	Sandy Clay Loam	10YR 7/3
Btg	82	Sandy Clay Loam	10YR 7/1
Bg	100+	Clay Loam	10YR 6/1

Additional Notes

Depth to grey redox depletions: 66 cm

Depth to redox iron concentrations: 0 cm

P6B20S3
Caroline County
Mapped Soil Series: Lenni

Horizon	Depth (cm)	Texture	Dominate Color
Ap	20	Sandy Loam	10YR 5/4
A	38	Clay Loam	10YR 5/4
Bg1	62	Clay Loam	10YR 6/2
Bg2	80	Sandy Clay Loam	10YR 7/1
Bg3	100+	Sandy Clay Loam	10YR 7/2

Additional Notes
Depth to grey redox depletions: 38 cm
Depth to redox iron concentrations: 38 cm

P6B0S1
Caroline County
Mapped Soil Series: Lenni

Horizon	Depth (cm)	Texture	Dominate Color
Ap	20	Silty Clay Loam	10YR 5/3
A	30	Sandy Clay Loam	10YR 5/3
Bg1	38	Silty Clay Loam	10YR 7/1
Bg2	100+	Clay Loam	10YR 7/1

Additional Notes
Depth to grey redox depletions: 30 cm
Depth to redox iron concentrations: 30 cm

P6B0S2
Caroline County
Mapped Soil Series: Lenni

Horizon	Depth (cm)	Texture	Dominate Color
Ap	20	Sandy Loam	10YR 5/3
A	32	Sandy Clay Loam	10YR 5/3
Bg1	40	Silty Clay Loam	10YR 6/1
Bg2	100+	Silty Clay Loam	10YR 7/1

Additional Notes
Depth to grey redox depletions: 32 cm
Depth to redox iron concentrations: 40 cm

P6B0S3
Caroline County
Mapped Soil Series: Lenni

Horizon	Depth (cm)	Texture	Dominate Color
Ap	20	Sandy Loam	7.5YR 4/2
A	52	Silty Loam	7.5YR 4/2
Bg	66	Silty Loam	10YR 7/1
Btg1	89	Clay Loam	10YR 6/1
Btg2	100+	Silty Clay Loam	10YR 6/1

Additional Notes
Depth to grey redox depletions: 52 cm
Depth to redox iron concentrations: 65 cm

P3B25S1
Queen Anne's County
Mapped Soil Series: Hammonton

Horizon	Depth (cm)	Texture	Dominate Color
Ap1	20	Sandy Clay Loam	10YR 4/4
Ap2	40	Sandy Loam	10YR 4/4
B1	52	Sandy Clay Loam	10YR 4/6
B2	85	Sandy Loam	10YR 6/6
B3	100+	Sandy Clay Loam	7.5YR 6/8

Additional Notes
Depth to redox iron concentrations: 84 cm

P3B25S2
Queen Anne's County
Mapped Soil Series: Hammonton

Horizon	Depth (cm)	Texture	Dominate Color
Ap	20	Sandy Loam	10YR 4/3
A	40	Sandy Clay Loam	10YR 4/3
B1	60	Sandy Clay Loam	10YR 4/4
B2	100+	Clay Loam	10YR 5/4

P3B25S3
Queen Anne's County
Mapped Soil Series: Hammonton

Horizon	Depth (cm)	Texture	Dominate Color
Ap	32	Sandy Loam	10YR 4/4
B1	80	Sandy Loam	10YR 4/6
B2	100+	Sandy Loam	10YR 6/6

P3B26S1
Queen Anne's County
Mapped Soil Series: Hammonton

Horizon	Depth (cm)	Texture	Dominate Color
Ap	20	Loam	10YR 4/4
A	40	Sandy Clay Loam	10YR 4/4
B1	51	Sandy Clay Loam	10YR 3/4
B2	80	Sandy Clay Loam	10YR 5/4
Bt	100+	Sandy Clay Loam	10YR 5/6

P3B26S2
Queen Anne's County
Mapped Soil Series: Hammonton

Horizon	Depth (cm)	Texture	Dominate Color
Ap	30	Sandy Loam	10YR 4/4
B1	58	Sandy Clay Loam	10YR 5/4
B2	76	Sandy Clay Loam	10YR 5/6
Bt	100+	Sandy Clay Loam	10YR 6/8

Additional Notes
Depth to redox iron concentrations: 76 cm

P3B26S3
Queen Anne's County
Mapped Soil Series: Hammonton

Horizon	Depth (cm)	Texture	Dominate Color
Ap	20	Sandy Loam	10YR 4/4
A	40	Clay Loam	10YR 4/4
B1	90	Sandy Clay Loam	10YR 5/4
B2	100+	Sandy Clay Loam	10YR 6/6

Additional Notes
Depth to redox iron concentrations: 90 cm

P2B2S1
Caroline County
Mapped Soil Series: Woodstown

Horizon	Depth (cm)	Texture	Dominate Color
Ap	20	Clay Loam	10YR 4/2
A	50	Silty Clay Loam	10YR 4/2
Btg	80	Clay Loam	10YR 5/1
Bt	100+	Silty Clay Loam	10YR 3/2

Additional Notes
2 subsurface pipes draining this bay
Depth to grey redox depletions: 0 cm
Depth to redox iron concentrations: 0 cm
No hydric soil indicators – insufficient redox iron concentrations in Ap for F3

P2B2S2
Caroline County
Mapped Soil Series: Woodstown

Horizon	Depth (cm)	Texture	Dominate Color
Ap	13	Sandy Clay Loam	10YR 5/2
Btg1	70	Silty Clay Loam	10YR 6/1
Btg2	92	Silty Clay Loam	10YR 7/1
Btg3	100+	Sandy Clay Loam	10YR 7/1

Additional Notes
2 subsurface pipes draining this bay
Depth to grey redox depletions: 0 cm
Depth to redox iron concentrations: 0 cm

P2B2S3
Caroline County
Mapped Soil Series: Woodstown

Horizon	Depth (cm)	Texture	Dominate Color
Ap	20	Sandy Clay Loam	10YR 5/2
A	33	Clay Loam	10YR 5/2
Btg1	53	Clay Loam	10YR 7/1
Btg2	100+	Silty Clay Loam	10YR 7/1

Additional Notes
2 subsurface pipes draining this bay
Depth to grey redox depletions: 0 cm

P2B10S1
Caroline County
Mapped Soil Series: Lenni

Horizon	Depth (cm)	Texture	Dominate Color
Ap	29	Sandy Clay Loam	10YR 5/2
Btg1	58	Sandy Clay Loam	10YR 6/2
Bg	100+	Loamy Sand	10YR 7/1

Additional Notes
Depth to grey redox depletions: 29 cm
Depth to redox iron concentrations: 29 cm

P2B10S2
Caroline County
Mapped Soil Series: Lenni

Horizon	Depth (cm)	Texture	Dominate Color
Ap	20	Loam	10YR 5/2
A	40	Sandy Clay Loam	10YR 5/2
Btg1	58	Clay Loam	10YR 7/1
Btg2	81	Silty Clay Loam	10YR 7/1
Btg3	100+	Silty Clay Loam	10YR 6/1

Additional Notes
Depth to grey redox depletions: 40 cm
Depth to redox iron concentrations: 58 cm

P2B10S3
Caroline County
Mapped Soil Series: Lenni

Horizon	Depth (cm)	Texture	Dominate Color
Ap	20	Clay Loam	10YR 4/2
A	35	Silty Clay Loam	10YR 4/2
Btg1	61	Clay Loam	10YR 7/1
Btg2	100+	Silty Clay Loam	10YR 7/1

Additional Notes
Depth to grey redox depletions: 35 cm
Depth to redox iron concentrations: 61 cm

P2B14S1
Caroline County
Mapped Soil Series: Ingleside

Horizon	Depth (cm)	Texture	Dominate Color
Ap	48	Sandy Loam	10YR 5/2
B	68	Sandy Clay Loam	10YR 3/3
Bg	100+	Sandy Clay Loam	10YR 7/1

Additional Notes
Depth to grey redox depletions: 65 cm
Depth to redox iron concentrations: 20 cm

P2B14S2
Caroline County
Mapped Soil Series: Ingleside

Horizon	Depth (cm)	Texture	Dominate Color	Notes
Ap	20	Sandy Loam	10YR 4/2	
A	62	Sandy Clay Loam	10YR 4/2	Pieces of darker soil (10YR 2/2) appear in this layer starting at 55 cm
Bg	100+	Loamy Sand	10YR 7/1	

Additional Notes
Depth to grey redox depletions: 62 cm
Depth to redox iron concentrations: 62 cm

P2B14S3
Caroline County
Mapped Soil Series: Ingleside

Horizon	Depth (cm)	Texture	Dominate Color
Ap	39	Sandy Clay Loam	10YR 4/2
B	50	Sandy Clay Loam	10YR 3/2
Bg	100+	Sandy Loam	10YR 7/1

Additional Notes
Depth to grey redox depletions: 51 cm
Depth to redox iron concentrations: 51 cm

P2B11S1
Caroline County
Mapped Soil Series: Ingleside

Horizon	Depth (cm)	Texture	Dominate Color
Ap	53	Silty Clay Loam	10YR 5/3
Btg	100+	Sandy Clay Loam	10YR 7/1

Additional Notes
Depth to grey redox depletions: 53 cm
Depth to redox iron concentrations: 0 cm

P2B11S2
Caroline County
Mapped Soil Series: Ingleside

Horizon	Depth (cm)	Texture	Dominate Color
Ap	20	Sandy Clay Loam	10YR 5/2
A	33	Silty Clay Loam	10YR 5/2
Bt	60	Silty Clay Loam	10YR 5/3
Btg	100+	Clay Loam	10YR 7/1

Additional Notes
Depth to grey redox depletions: 60 cm
Depth to redox iron concentrations: 60 cm

P2B11S3
Caroline County
Mapped Soil Series: Ingleside

Horizon	Depth (cm)	Texture	Dominate Color
Ap	20	Silty Clay Loam	10YR 5/2
A	60	Silt Loam	10YR 5/2
Bt	70	Sandy Clay Loam	10YR 5/2
Btg	100+	Clay Loam	10YR 7/1

Additional Notes
Depth to grey redox depletions: 70 cm
Depth to redox iron concentrations: 70 cm

P2B12S1
Caroline County
Mapped Soil Series: Woodstown

Horizon	Depth (cm)	Texture	Dominate Color
Ap	23	Sandy Loam	10YR 5/3
B1	53	Sandy Loam	10YR 6/4
B2	100+	Sandy Clay Loam	10YR 6/4

Additional Notes
Depth to redox iron concentrations: 23 cm

P2B12S2
Caroline County
Mapped Soil Series: Woodstown

Horizon	Depth (cm)	Texture	Dominate Color
Ap	33	Sandy Clay Loam	10YR 5/2
B1	80	Sandy Clay Loam	10YR 7/1
B2	100+	Sandy Loam	2.5Y 7/1

Additional Notes
Depth to grey redox depletions: 33 cm
Depth to redox iron concentrations: 33 cm

P2B12S3
Caroline County
Mapped Soil Series: Woodstown

Horizon	Depth (cm)	Texture	Dominate Color
Ap	20	Sandy Loam	10YR 5/2
A	48	Sandy Clay Loam	10YR 5/2
Bg	74	Sandy Clay Loam	10YR 7/1
Btg	100+	Sandy Clay Loam	10YR 6/1

Additional Notes
Depth to grey redox depletions: 48 cm
Depth to redox iron concentrations: 48 cm

P2B13S1
Caroline County
Mapped Soil Series: Ingleside

Horizon	Depth (cm)	Texture	Dominate Color
Ap	40	Sandy Loam	10YR 5/2
Btg1	71	Clay Loam	2.5Y 5/2
Btg2	89	Clay Loam	10YR 7/1
Bg	100+	Sandy Clay Loam	2.5Y 6/1

Additional Notes
Depth to grey redox depletions: 40 cm
Depth to redox iron concentrations: 40 cm

P2B13S2
Caroline County
Mapped Soil Series: Ingleside

Horizon	Depth (cm)	Texture	Dominate Color
Ap	31	Sandy Loam	10YR 5/2
Btg1	56	Sandy Clay Loam	10YR 6/1
Btg2	100+	Sandy Clay Loam	2.5Y 7/1

Additional Notes
Depth to grey redox depletions: 31 cm
Depth to redox iron concentrations: 31 cm

P2B13S3
Caroline County
Mapped Soil Series: Ingleside

Horizon	Depth (cm)	Texture	Dominate Color
Ap	36	Sandy Loam	10YR 5/2
Btg1	60	Sandy Clay Loam	10YR 7/1
Btg2	80	Sandy Clay Loam	2.5Y 6/1
Bg	100+	Sandy Loam	2.5Y 6/1

Additional Notes
Depth to grey redox depletions: 36 cm
Depth to redox iron concentrations: 36 cm

P2B24S1
Caroline County
Mapped Soil Series: Corsica

Horizon	Depth (cm)	Texture	Dominate Color
Ap1	20	Sandy Clay Loam	10YR 2/1
Ap2	40	Silty Clay Loam	10YR 2/1
Bt	54	Silty Clay Loam	10YR 4/1
Btg	100+	Silty Clay Loam	2.5Y 7/1

Additional Notes
Two ditches running through this bay
Depth to grey redox depletions: 54 cm
Depth to redox iron concentrations: 54 cm
Depth to freestanding water: 26 cm

P2B24S2
Caroline County
Mapped Soil Series: Corsica

Horizon	Depth (cm)	Texture	Dominate Color
Ap1	20	Sandy Loam	10YR 2/1
Ap2	32	Sandy Clay Loam	10YR 2/1
B	54	Sandy Clay Loam	10YR 3/1
Bt	75	Sandy Clay Loam	10YR 4/1
Bg	100+	Sandy Loam	10YR 7/1

Additional Notes
Two ditches running through this bay
Depth to grey redox depletions: 53 cm
Depth to redox iron concentrations: 53 cm
Depth to freestanding water: 27 cm

P2B24S3
Caroline County
Mapped Soil Series: Corsica

Horizon	Depth (cm)	Texture	Dominate Color
Ap	42	Sandy Clay Loam	10YR 3/1
B	64	Silty Clay Loam	2.5Y 2.5/1
Bt1	88	Silty Clay Loam	2.5Y 3/1
Bt2	100+	Sandy Clay Loam	10YR 4/1

Additional Notes
Two ditches running through this bay
Depth to freestanding water: 34 cm

P2B1S1
Caroline County
Mapped Soil Series: Lenni

Horizon	Depth (cm)	Texture	Dominate Color
Ap	37	Sandy Clay Loam	10YR 5/2
Bg	62	Silty Clay Loam	10YR 7/1
Btg1	86	Silty Clay Loam	10YR 6/1
Btg2	100+	Clay Loam	2.5Y 7/1

Additional Notes
One underground pipe drains this bay
Depth to grey redox depletions: 37 cm
Depth to redox iron concentrations: 63 cm

P2B1S2
Caroline County
Mapped Soil Series: Lenni

Horizon	Depth (cm)	Texture	Dominate Color
Ap	20	Sandy Clay Loam	10YR 5/2
A	31	Clay Loam	10YR 5/2
Bg	51	Silty Clay Loam	10YR 7/1
Btg	100+	Silty Clay Loam	2.5Y 7/1

Additional Notes
One underground pipe drains this bay
Depth to grey redox depletions: 31 cm
Depth to redox iron concentrations: 51 cm
Depth to freestanding water: 33 cm

P2B1S3
Caroline County
Mapped Soil Series: Lenni

Horizon	Depth (cm)	Texture	Dominate Color
Ap	20	Silty Clay Loam	10YR 5/2
A	33	Sandy Clay Loam	10YR 5/2
Bg	83	Clay Loam	10YR 7/1
Btg	100+	Silty Clay Loam	2.5Y 7/1

Additional Notes
One underground pipe drains this bay
Depth to grey redox depletions: 33 cm
Depth to redox iron concentrations: 33 cm

P5B3S1
Caroline County
Mapped Soil Series: Hurlock

Horizon	Depth (cm)	Texture	Dominate Color
Ap	20	Sandy Loam	10YR 5/2
A	37	Sandy Clay Loam	10YR 5/2
Bg1	53	Sandy Clay Loam	2.5Y 5/2
Bg2	74	Sandy Clay Loam	2.5Y 6/1
Bg3	100+	Sandy Clay Loam	2.5Y 7/1

Additional Notes
Depth to grey redox depletions: 65 cm
Depth to redox iron concentrations: 37 cm

P5B3S2
Caroline County
Mapped Soil Series: Hurlock

Horizon	Depth (cm)	Texture	Dominate Color
Ap	20	Sandy Loam	10YR 5/2
A	32	Sandy Clay Loam	10YR 5/2
Btg	72	Clay Loam	10YR 7/1
Bg1	81	Sandy Loam	10YR 7/1
Bg2	92	Loamy Sand	10YR 7/2
B	100+	Loamy Sand	10YR 4/6

Additional Notes
Depth to grey redox depletions: 32 cm
Depth to redox iron concentrations: 32 cm

P5B3S3
Caroline County
Mapped Soil Series: Hurlock

Horizon	Depth (cm)	Texture	Dominate Color
Ap	32	Sandy Clay Loam	10YR 5/2
B	45	Sandy Clay Loam	2.5Y 5/2
Bg1	58	Sandy Clay Loam	2.5Y 7/1
Bg2	72	Sandy Loam	2.5Y 6/2
Bg3	100+	Sandy Loam	2.5Y 7/2

Additional Notes
Depth to grey redox depletions: 45 cm
Depth to redox iron concentrations: 58 cm

P5B4S1
Caroline County
Mapped Soil Series: Ingleside

Horizon	Depth (cm)	Texture	Dominate Color
Ap	20	Sandy Loam	10YR 4/3
A	28	Sandy Clay Loam	10YR 4/3
Bt	75	Sandy Clay Loam	10YR 5/2
Bg	100+	Sandy Loam	10YR 6/2

Additional Notes
Depth to redox iron concentrations: 55 cm

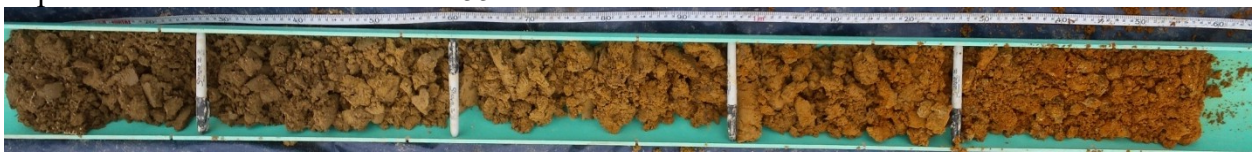

P5B4S2
Caroline County
Mapped Soil Series: Ingleside

Horizon	Depth (cm)	Texture	Dominate Color
Ap	39	Sandy Clay Loam	10YR 5/3
Bg	55	Sandy Clay Loam	10YR 5/2
B1	87	Sandy Clay Loam	10YR 6/3
B2	100+	Sandy Clay Loam	10YR 7/3

Additional Notes
Depth to redox iron concentrations: 39 cm

P5B4S3
Caroline County
Mapped Soil Series: Ingleside

Horizon	Depth (cm)	Texture	Dominate Color
Ap	20	Sandy Loam	10YR 4/3
A	28	Sandy Clay Loam	10YR 4/3
B	46	Sandy Clay Loam	2.5Y 5/4
Btg	84	Sandy Clay Loam	10YR 5/2
Bg	100+	Sandy Loam	10YR 5/2

Additional Notes
Depth to redox iron concentrations: 46 cm

P5B29S1
Caroline County
Mapped Soil Series: Hurlock

Horizon	Depth (cm)	Texture	Dominate Color
Ap	34	Sandy Clay Loam	10YR 4/2
Btg	40	Sandy Clay Loam	10YR 6/1
Bg	60	Silty Clay Loam	10YR 7/1
Btg	100+	Silty Clay Loam	10YR 5/1

Additional Notes
Depth to grey redox depletions: 34 cm
Depth to redox iron concentrations: 55 cm

P5B29S2
Caroline County
Mapped Soil Series: Hurlock

Horizon	Depth (cm)	Texture	Dominate Color
Ap	31	Sandy Clay Loam	10YR 5/2
Bg1	45	Sandy Clay Loam	2.5Y 6/1
Bg2	90	Loamy Sand	2.5Y 5/1
Bg3	100+	Sandy Clay Loam	2.5Y 5/1

Additional Notes
Depth to grey redox depletions: 31 cm
Depth to redox iron concentrations: 44 cm

P5B29S3
Caroline County
Mapped Soil Series: Hurlock

Horizon	Depth (cm)	Texture	Dominate Color
Ap	21	Clay Loam	10YR 5/2
Bg1	31	Sandy Clay Loam	2.5Y 6/1
Bg2	55	Silty Clay Loam	2.5Y 5/2
Btg1	67	Clay Loam	10YR 6/1
Btg2	100+	Silty Clay Loam	10YR 7/1

Additional Notes
Depth to grey redox depletions: 21 cm
Depth to redox iron concentrations: 31 cm

P5B9S1
Caroline County
Mapped Soil Series: Woodstown

Horizon	Depth (cm)	Texture	Dominate Color
Ap	23	Sandy Clay Loam	10YR 5/2
B	48	Sandy Clay Loam	2.5Y 5/2
Bg1	88	Sandy Clay Loam	10YR 6/1
Bg2	100+	Sandy Clay Loam	2.5Y 6/1

Additional Notes
Depth to grey redox depletions: 48 cm
Depth to redox iron concentrations: 48 cm
Depth to freestanding water: 0.5 cm above the surface

P5B9S2
Caroline County
Mapped Soil Series: Woodstown

Horizon	Depth (cm)	Texture	Dominate Color
Ap	31	Sandy Clay Loam	2.5Y 5/2
Bg1	52	Clay Loam	2.5Y 6/2
Bg2	87	Sandy Clay Loam	10YR 6/1
Bgt	100+	Clay Loam	10YR 6/1

Additional Notes
Depth to grey redox depletions: 31 cm
Depth to redox iron concentrations: 87 cm
Depth to freestanding water: 29 cm

P5B9S3
Caroline County
Mapped Soil Series: Woodstown

Horizon	Depth (cm)	Texture	Dominate Color
Ap	20	Loam	10YR 5/2
A	32	Clay Loam	10YR 6/2
Btg	89	Sandy Clay Loam	10YR 6/1
Bg	100+	Sandy Loam	10YR 6/1

Additional Notes
Depth to grey redox depletions: 32 cm
Depth to redox iron concentrations: 32 cm
Depth to freestanding water: 40 cm

P5B6S1
Caroline County
Mapped Soil Series: Ingleside

Horizon	Depth (cm)	Texture	Dominate Color
Ap	20	Sandy Clay Loam	10YR 5/2
A	56	Silty Clay Loam	10YR 5/2
Btg	93	Sandy Clay Loam	2.5Y 6/1
Bg	100+	Sandy Loam	2.5Y 6/1

Additional Notes
Depth to grey redox depletions: 56 cm
Depth to freestanding water: 24 cm

P5B6S2
Caroline County
Mapped Soil Series: Ingleside

Horizon	Depth (cm)	Texture	Dominate Color
Ap	34	Loam	10YR 5/2
Btg	62	Clay Loam	10YR 7/1
Bg	100+	Sandy Loam	7.5YR 6/1

Additional Notes
Depth to grey redox depletions: 42 cm
Depth to redox iron concentrations: 62 cm

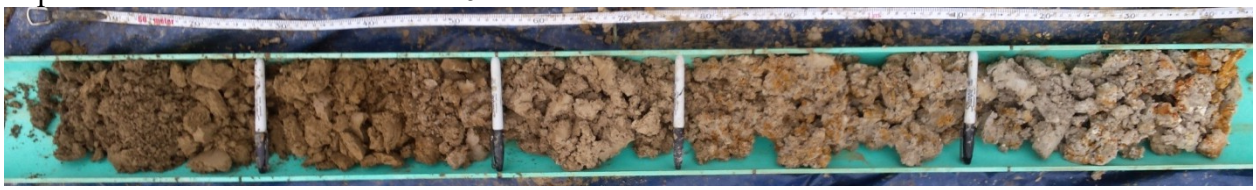

P5B6S3
Caroline County
Mapped Soil Series: Ingleside

Horizon	Depth (cm)	Texture	Dominate Color
Ap	20	Clay Loam	10YR 5/2
A	31	Sandy Clay Loam	10YR 5/2
Btg	69	Sandy Clay Loam	10YR 6/1
Bg1	80	Sandy Clay Loam	10YR 7/1
Bg2	100+	Sandy Loam	10YR 7/1

Additional Notes
Depth to grey redox depletions: 31 cm
Depth to redox iron concentrations: 31 cm

P5B5S1
Caroline County
Mapped Soil Series: Woodstown

Horizon	Depth (cm)	Texture	Dominate Color
Ap	20	Sandy Loam	10YR 5/2
A	33	Sandy Clay Loam	10YR 5/2
B	70	Sandy Clay Loam	2.5Y 6/3
Bg	100+	Sandy Clay Loam	10YR 7/1

Additional Notes
Depth to grey redox depletions: 70 cm
Depth to redox iron concentrations: 33 cm

P5B5S2
Caroline County
Mapped Soil Series: Woodstown

Horizon	Depth (cm)	Texture	Dominate Color
Ap	20	Sandy Clay Loam	10YR 5/2
A	31	Sandy Loam	10YR 5/2
Btg	71	Sandy Clay Loam	10YR 6/2
Bg	100+	Sandy Clay Loam	10YR 7/2

Additional Notes
Depth to grey redox depletions: 31 cm
Depth to redox iron concentrations: 31 cm
Depth to freestanding water: 59 cm

P5B5S3
Caroline County
Mapped Soil Series: Woodstown

Horizon	Depth (cm)	Texture	Dominate Color
Ap	20	Loam	10YR 5/2
A	30	Sandy Clay Loam	10YR 5/2
Bg1	66	Sandy Clay Loam	10YR 5/1
Bg2	100+	Sandy Cay Loam	10YR 7/1

Additional Notes
Depth to grey redox depletions: 30 cm
Depth to redox iron concentrations: 30 cm
Depth to freestanding water: 66 cm

P5B8S1
Caroline County
Mapped Soil Series: Galestown

Horizon	Depth (cm)	Texture	Dominate Color
Ap	20	Loamy Sand	10YR 4/2
A	27	Sandy Loam	10YR 4/2
Bg1	40	Sandy Loam	10YR 5/1
Bg2	70	Sandy Loam	2.5Y 6/1
Bg3	100+	Sandy Loam	2.5Y 7/1

Additional Notes
Depth to grey redox depletions: 27 cm

P5B8S2
Caroline County
Mapped Soil Series: Galestown

Horizon	Depth (cm)	Texture	Dominate Color
Ap	31	Sandy Loam	10YR 3/2
Bg1	40	Loamy Sand	2.5Y 6/2
Bg2	100+	Loamy Sand	2.5Y 7/2

Additional Notes
Depth to grey redox depletions: 31 cm

P5B8S3
Caroline County
Mapped Soil Series: Galestown

Horizon	Depth (cm)	Texture	Dominate Color
Ap	43	Sandy Loam	10YR 3/2
Bg1	66	Loamy Sand	2.5YR 6/1
Bg2	100+	Sandy Loam	2.5Y 7/1

Additional Notes
Depth to grey redox depletions: 43 cm

P5B7S1
Caroline County
Mapped Soil Series: Ingleside

Horizon	Depth (cm)	Texture	Dominate Color
Ap	20	Sandy Loam	10YR 5/2
A	38	Sandy Clay Loam	10YR 5/2
Bg	68	Sandy Clay Loam	2.5Y 6/1
Btg	100+	Sandy Loam	2.5Y 7/1

Additional Notes
Depth to grey redox depletions: 38 cm
Depth to redox iron concentrations: 38 cm

P5B7S2
Caroline County
Mapped Soil Series: Ingleside

Horizon	Depth (cm)	Texture	Dominate Color
Ap	20	Sandy Loam	10YR 4/2
A	40	Sandy Clay Loam	10YR 4/2
Bg	51	Sandy Clay Loam	2.5Y 6/2
Btg	100+	Sandy Loam	2.5Y 6/2

Additional Notes
Depth to grey redox depletions: 40 cm
Depth to redox iron concentrations: 51 cm

P5B7S3
Caroline County
Mapped Soil Series: Ingleside

Horizon	Depth (cm)	Texture	Dominate Color
Ap	42	Sandy Clay Loam	10YR 4/2
Bg	100+	Loamy Sand	10YR 7/1

Additional Notes
Depth to grey redox depletions: 42 cm
Depth to redox iron concentrations: 42 cm

P1B21S1
Caroline County
Mapped Soil Series: Fallingston

Horizon	Depth (cm)	Texture	Dominate Color
Ap	20	Silty Loam	10YR 2/2
A	43	Silty Clay Loam	10YR 2/2
Bt	53	Silty Clay Loam	10YR 2/1
Btg	100+	Silty Cay Loam	10YR 6/1

Additional Notes
One ditch draining this Bay
Depth to grey redox depletions: 53 cm
Depth to redox iron concentrations: 53 cm
Depth to freestanding water: 53 cm

P1B21S2
Caroline County
Mapped Soil Series: Fallingston

Horizon	Depth (cm)	Texture	Dominate Color
Ap	20	Sandy Loam	10YR 4/1
A	34	Sandy Clay Loam	10YR 4/1
B	60	Silty Clay Loam	10YR 3/1
Bt	80	Silty Clay Loam	2.5Y 2.5/1
Btg	100+	Silty Cay Loam	10YR 6/1

Additional Notes
One ditch draining this Bay
Depth to grey redox depletions: 80 cm
Depth to redox iron concentrations: 80 cm
Depth to freestanding water: 81 cm

P1B21S3
Caroline County
Mapped Soil Series: Fallingston

Horizon	Depth (cm)	Texture	Dominate Color
Ap	20	Clay Loam	10YR 3/1
A	51	Silty Clay Loam	10YR 3/1
B	69	Silty Clay Loam	10YR 2/1
Btg	100+	Silty Cay Loam	10YR 6/1

Additional Notes
One ditch draining this Bay
Depth to grey redox depletions: 69 cm
Depth to redox iron concentrations: 69 cm

P1B22S1
Caroline County
Mapped Soil Series: Hambrook

Horizon	Depth (cm)	Texture	Dominate Color
Ap	20	Clay Loam	10YR 4/1
A	41	Sandy Clay Loam	10YR 4/1
Bg1	58	Sandy Clay Loam	2.5Y 6/1
Bg2	73	Loamy Sand	2.5Y 6/1
Bg3	100+	Loamy Sand	2.5Y 7/1

Additional Notes
Tile drainage in this Bay
Depth to grey redox depletions: 41 cm
Depth to redox iron concentrations: 41 cm

P1B22S2
Caroline County
Mapped Soil Series: Sassafras

Horizon	Depth (cm)	Texture	Dominate Color
Ap	20	Clay Loam	10YR 4/1
A	32	Sandy Clay Loam	10YR 4/1
Btg	52	Clay Loam	10YR 6/1
Bg1	63	Sandy Clay Loam	10YR 6/1
Bg2	100+	Sandy Clay Loam	2.5Y 7/1

Additional Notes
Tile drainage in this Bay
Depth to grey redox depletions: 32 cm
Depth to redox iron concentrations: 32 cm

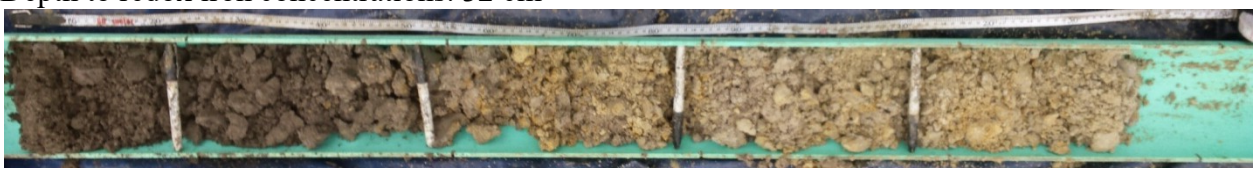

P1B22S3
Caroline County
Mapped Soil Series: Hambrook

Horizon	Depth (cm)	Texture	Dominate Color
Ap	45	Sandy Clay Loam	10YR 4/1
Btg1	59	Clay Loam	2.5Y 6/1
Btg2	72	Silty Clay Loam	10YR 6/1
Btg3	100+	Sandy Cay Loam	2.5Y 7/1

Additional Notes
Tile drainage in this Bay
Depth to grey redox depletions: 45 cm
Depth to redox iron concentrations: 45 cm

P1B16S1
Caroline County
Mapped Soil Series: Fallingston

Horizon	Depth (cm)	Texture	Dominate Color
Ap	20	Clay Loam	10YR 4/1
A	31	Silty Clay Loam	10YR 4/1
Btg1	57	Silty Clay Loam	2.5Y 5/1
Btg2	69	Clay Loam	2.5Y 6/1
Btg3	100+	Sandy Cay Loam	10YR 5/1

Additional Notes
Depth to grey redox depletions: 31 cm
Depth to redox iron concentrations: 69 cm

P1B16S2
Caroline County
Mapped Soil Series: Fallingston

Horizon	Depth (cm)	Texture	Dominate Color
Ap	20	Sandy Clay Loam	10YR 4/2
A	31	Sandy Loam	10YR 4/2
Bg1	51	Sandy Clay Loam	2.5Y 6/1
Bg2	76	Sandy Loam	10YR 7/1
Bg3	100+	Loamy Sand	2.5Y 7/2

Additional Notes
Depth to grey redox depletions: 31 cm
Depth to redox iron concentrations: 50 cm

P1B16S3
Caroline County
Mapped Soil Series: Fallingston

Horizon	Depth (cm)	Texture	Dominate Color
Ap	19	Sandy Clay Loam	2.5Y 5/2
A	41	Clay Loam	2.5Y 5/2
Btg	61	Sandy Clay Loam	2.5Y 7/1
Bg1	79	Sandy Loam	2.5Y 6/1
Bg2	100+	Loamy Sand	2.5Y 7/2

Additional Notes
Depth to grey redox depletions: 40 cm
Depth to redox iron concentrations: 40 cm

P1B15S1
Caroline County
Mapped Soil Series: Hambrook

Horizon	Depth (cm)	Texture	Dominate Color
Ap	36	Sandy Loam	10YR 4/2
B	61	Sandy Loam	10YR 5/3
Bg1	82	Sandy Clay Loam	10YR 5/2
Bg2	100+	Sandy Clay Loam	10YR 7/1

Additional Notes
Depth to grey redox depletions: 61 cm
Depth to redox iron concentrations: 61 cm

P1B15S2
Caroline County
Mapped Soil Series: Hambrook

Horizon	Depth (cm)	Texture	Dominate Color
Ap	20	Loam	10YR 4/2
A	37	Sandy Clay Loam	10YR 4/2
Bg	100+	Sandy Clay Loam	10YR 6/1

Additional Notes
Depth to grey redox depletions: 37 cm
Depth to redox iron concentrations: 37 cm

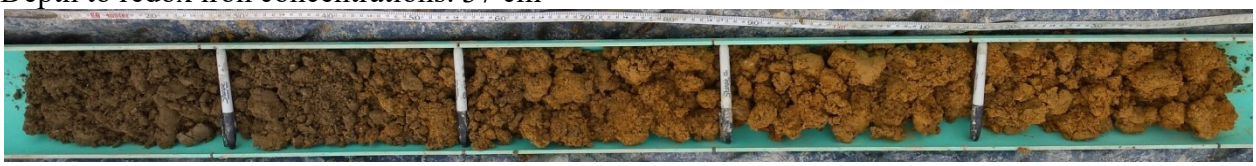

P1B15S3
Caroline County
Mapped Soil Series: Hambrook

Horizon	Depth (cm)	Texture	Dominate Color
Ap	20	Sandy Loam	10YR 5/2
A	41	Sandy Clay Loam	10YR 5/2
Bg1	78	Sandy Clay Loam	2.5Y 5/1
Bg2	100+	Sandy Clay Loam	2.5Y 6/2

Additional Notes
Depth to grey redox depletions: 41 cm
Depth to redox iron concentrations: 41 cm

P1B19S1
Caroline County
Mapped Soil Series: Lenni

Horizon	Depth (cm)	Texture	Dominate Color
Ap	20	Silty Clay Loam	10YR 4/1
A	34	Clay Loam	10YR 4/1
Btg1	46	Silty Clay Loam	10YR 7/1
Btg2	82	Silty Clay Loam	10YR 6/1
Bg	100+	Sandy Loam	2.5Y 7/1

Additional Notes
Depth to grey redox depletions: 34 cm
Depth to redox iron concentrations: 34 cm
Depth to freestanding water: 77 cm

P1B19S2
Caroline County
Mapped Soil Series: Lenni

Horizon	Depth (cm)	Texture	Dominate Color
Ap	20	Sandy Loam	10YR 4/1
A	34	Sandy Clay Loam	10YR 4/1
Btg1	69	Clay Loam	10YR 4/1
Btg2	100+	Silty Clay Loam	10YR 7/1

Additional Notes
Depth to grey redox depletions: 69 cm
Depth to redox iron concentrations: 34 cm
Depth to freestanding water: 9 cm

P1B19S3
Caroline County
Mapped Soil Series: Lenni

Horizon	Depth (cm)	Texture	Dominate Color
Ap	20	Sandy Loam	10YR 4/1
A	36	Sandy Clay Loam	10YR 4/1
Btg1	46	Sandy Clay Loam	10YR 2/1
Btg2	63	Sandy Clay Loam	10YR 4/1
Btg3	82	Silty Clay Loam	10YR 5/1
Bg	100+	Sandy Cay Loam	2.5Y 6/1

Additional Notes
Depth to grey redox depletions: 63 cm
Depth to freestanding water: 76 cm

P1B18S1
Caroline County
Mapped Soil Series: Hambrook

Horizon	Depth (cm)	Texture	Dominate Color
Ap	20	Silty Loam	10YR 5/2
A	37	Loamy Sand	10YR 5/2
B	73	Sandy Loam	10YR 5/3
Bg	100+	Loamy Sand	10YR 7/2

Additional Notes
Depth to grey redox depletions: 73 cm
Depth to redox iron concentrations: 37 cm

P1B18S2
Caroline County
Mapped Soil Series: Hambrook

Horizon	Depth (cm)	Texture	Dominate Color
Ap	20	Silty Clay Loam	10YR 4/3
A	37	Loam	10YR 4/3
B	62	Sandy Clay Loam	2.5Y 5/3
Bg1	86	Silty Cay Loam	10YR 5/1
Bg2	100+	Sandy Clay Loam	10YR 5/1

Additional Notes
Depth to grey redox depletions: 62 cm
Depth to redox iron concentrations: 40 cm

P1B18S3
Caroline County
Mapped Soil Series: Hambrook

Horizon	Depth (cm)	Texture	Dominate Color
Ap	20	Clay Loam	10YR 4/3
A	40	Silt Loam	10YR 4/3
Bg	64	Clay Loam	10YR 6/1
Btg	100+	Sandy Cay Loam	2.5Y 6/1

Additional Notes
Depth to grey redox depletions: 40 cm
Depth to redox iron concentrations: 40 cm

P1B17S1
Caroline County
Mapped Soil Series: Sassafras

Horizon	Depth (cm)	Texture	Dominate Color
Ap	20	Sandy Loam	10YR 4/2
A	40	Sandy Clay Loam	10YR 4/2
Bg1	67	Sandy Loam	2.5Y 5/2
Bg2	100+	Loamy Sand	2.5Y 5/2

Additional Notes
Depth to grey redox depletions: 67 cm
Depth to redox iron concentrations: 67 cm

P1B17S2
Caroline County
Mapped Soil Series: Fallingston

Horizon	Depth (cm)	Texture	Dominate Color
Ap	20	Clay Loam	10YR 4/2
A	43	Sandy Clay Loam	10YR 4/2
Bg1	73	Sandy Clay Loam	10YR 6/1
Bg2	100+	Sandy Cay Loam	10YR 7/1

Additional Notes
Depth to grey redox depletions: 43 cm
Depth to redox iron concentrations: 43 cm

P1B17S3
Caroline County
Mapped Soil Series: Sassafras

Horizon	Depth (cm)	Texture	Dominate Color
Ap	20	Clay Loam	10YR 4/2
A	50	Sandy Loam	10YR 4/2
Bg1	82	Sandy Clay Loam	10YR 5/1
Bg2	91	Sandy Loam	10YR 6/1
Btg	100+	Sandy Clay Loam	2.5Y 7/1

Additional Notes
Depth to grey redox depletions: 70 cm
Depth to redox iron concentrations: 60 cm

P1B28S1
Caroline County
Mapped Soil Series: Lenni

Horizon	Depth (cm)	Texture	Dominate Color	Notes
Ap	20	Sandy Loam	2.5Y 4/2	
A	36	Sandy Clay Loam	2.5Y 4/2	
Bg1	53	Sandy Clay Loam	10YR 5/1	
Bg2	68	Sandy Loam	10YR 5/1	Seashell fragments present
Bg3	100+	Sandy Loam	10YR 6/1	

Additional Notes
Depth to grey redox depletions: 36 cm
Depth to redox iron concentrations: 36 cm

P1B28S2
Caroline County
Mapped Soil Series: Lenni

Horizon	Depth (cm)	Texture	Dominate Color	Notes
Ap	20	Sandy Clay Loam	10YR 4/2	
A	38	Sandy Loam	10YR 4/2	
Btg1	64	Sandy Clay Loam	2.5Y 6/1	
Btg2	100+	Sandy Clay Loam	2.5Y 7/1	Seashell fragments present

Additional Notes
Depth to grey redox depletions: 38 cm
Depth to redox iron concentrations: 38 cm

P1B28S3
Caroline County
Mapped Soil Series: Lenni

Horizon	Depth (cm)	Texture	Dominate Color
Ap	20	Sandy Loam	2.5Y 4/2
A	42	Sandy Clay Loam	2.5Y 4/2
Bg1	72	Silty Clay Loam	2.5Y 6/1
Bg2	85	Sandy Clay Loam	2.5Y 6/1
Bg3	100+	Sandy Clay Loam	2.5Y 7/1

Additional Notes
Depth to grey redox depletions: 42 cm
Depth to redox iron concentrations: 42 cm